## **Self Assembled Cages with Mechanically Interlocked Cucurbiturils**

Kimberly G. Brady, † Bingqing Liu, ‡ Xiaopeng Li, ‡ and Lyle Isaacs\*†

<sup>†</sup>Department of Chemistry and Biochemistry, University of Maryland, College Park, Maryland 20742, United States; <sup>‡</sup>Department of Chemistry, University of South Florida, Tampa, Florida 33620, United States

 $\hbox{\tt *To whom correspondence should be addressed. Prof. Lyle Isaacs, Email: LIsaacs@umd.edu}\\$ 

**Abstract:** We report preparation of (bis)aniline ligand 4 which contains a central viologen binding domain and its subcomponent self-assembly with aldehyde 5 and Fe(OTf)<sub>2</sub> in CH<sub>3</sub>CN to yield tetrahedral assembly 6. Complexation of ligand 4 with CB[7] in the form of CB[7]•4•2PF<sub>6</sub> allows the preparation of assembly 7 which contains an average of 1.95 (range 1-3) mechanically interlocked CB[7] units. Assemblies 6 and 7 are hydrolytically unstable in water due to their imine linkages. Redesign of our system with water stable 2,2'-bipyridine end groups was realized in the form of ligands 11 and 16 which also contain a central viologen binding domain. Self-assembly of 11 with Fe(NTf<sub>2</sub>)<sub>2</sub> gave tetrahedral MOP 12 as evidenced by <sup>1</sup>H NMR, DOSY, and mass spectrometric analysis. In contrast, isomeric ligand 16 underwent self-assembly with Fe(OTf)<sub>2</sub> to give cubic assembly 17. Precomplexation of ligands 11 and 16 with CB[7] gave the acetonitrile soluble CB[7]•11•2PF<sub>6</sub> and CB[7]•16•2PF<sub>6</sub> complexes. Self-assembly of CB[7]•11•2PF<sub>6</sub> with Fe(OTf)<sub>2</sub> gave tetrahedron 13 which contains on average 1.8 mechanically interlocked CB[7] units as determined by <sup>1</sup>H NMR, DOSY, and ESI-MS analysis. Self-assembly of CB[7]•16•2PF<sub>6</sub> with Fe(OTf)<sub>2</sub> gave cube 13 which contains 6.59 mechanically interlocked CB[7] units as determined by <sup>1</sup>H NMR and DOSY measurements.

Keywords: Cucurbit[n]uril; metal organic polyhedra; self-assembly; mechanical interlocked compounds

Introduction. A wide variety of molecular container compounds have been studied over the past decades including cyclodextrins, cyclophanes, calixarenes, cavitands, and more recently cucurbit[n]uril (CB[n]) and pillararenes (Figure 1).(1) When molecular containers bind guest compounds within their cavity, they can fundamentally alter their optical properties (e.g. UV/Vis, fluorescence), physical properties (e.g. solubility, vapor pressure), chemical properties (e.g. conformation, reactivity, pKa), and even their biological properties.(2) Accordingly, molecular containers have been used in numerous applications including as supramolecular catalysts, as components of separations processes, as components of sensing ensembles, as components of smart materials and molecular machines, and to construct drug delivery systems.(3) Amongst these molecular containers, cyclodextrin derivatives have found a wide variety of practical real world applications including the formulation of insoluble pharmaceuticals for human use, as the active ingredient in the household product Febreeze<sup>TM</sup>, and as an *in vivo* reversal agent for rocuronium and vecuronium in the form of Sugammadex.(4)

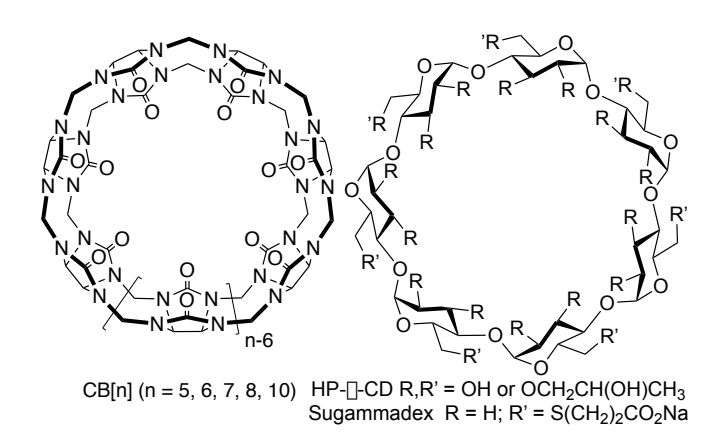


*Figure 1.* Structures of cyclodextrins and cucurbit[n]urils.

Our group has been most interested in the chemistry of the CB[n] family of molecular container compounds (Figure 1).(5) CB[n] are composed of n glycoluril repeat units connected by 2n

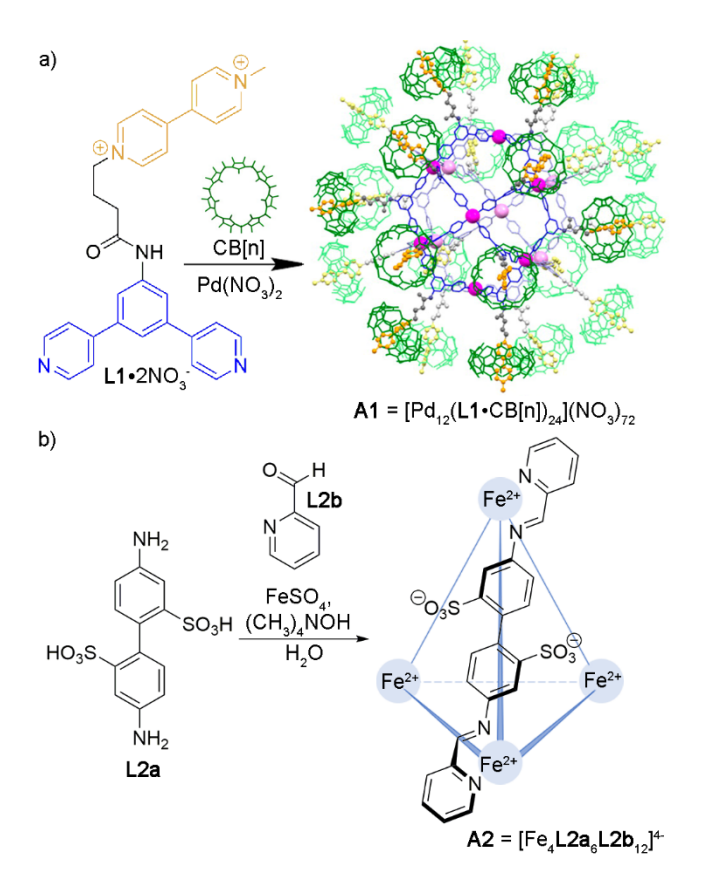
methylene bridges which define a central hydrophobic cavity and two symmetry equivalent ureidyl carbonyl portals that are regions of highly negative electrostatic potential.(6) Accordingly, CB[n] hosts bind to a wide variety of guest molecules that present hydrophobic and cationic functionality including the N-terminus of peptides and proteins, cationic dyes, alkyl and aryl (di)ammonium ions, neurotransmitters, active pharmaceutical ingredients, drugs of abuse, and electrochemically active guests like ferrocene and viologen derivatives.(7) Advantageously, CB[n]-type receptors typically display high in vitro and in vivo biocompatibility.(8) Compared to other molecular containers, CB[n]-type hosts are special because they display high affinity and highly selective binding events in water (K<sub>a</sub> commonly 10<sup>6</sup> M<sup>-1</sup>; K<sub>a</sub> up to 10<sup>17</sup> M<sup>-1</sup>).(5d,9) Because CB[n]•guest complexes are so selective they are responsive toward chemical, pH, photochemical, and electrochemical stimuli.(7i,7j,10) For all these reasons, CB[n]-type containers have been used in a variety of applications including chemical sensing, promotors of protein dimerization, drug formulation, delivery and sequestration, separations materials, and to construct molecular machines and devices.(5d,7c,11) CB[n] are even beginning to appear in household deodorizing products.(12)

Self-assembly processes driven by hydrogen bonding,(13) the hydrophobic effect,(14) or metal-ligand interactions(15) represent powerful alternative approaches toward functional molecular container compounds. Metal-ligand coordination-driven self-assembly has been particularly widely employed due to the well defined geometry of the metal coordination sphere and the strength of the metal-ligand interactions which lead to more predictable self-assembly processes. The vibrant fields of metal organic frameworks (MOF) and metal organic cages fall within the category of molecular containers self-assembled via metal-ligand interactions. MOFs are extended

solids that have been used for a variety of applications including as materials for hydrogen storage, water and gas capture and separation, carbon capture and sequestration, biological imaging and sensing, and drug delivery processes.(15d,16) The Loeb and Stoddart groups have studied the incorporation of macrocycles into MOFs and studied their dynamic and host-guest recognition properties.(17) Related supramolecular organic frameworks (SOFs) incorporating CB[n] have been developed in recent years by the Li group.(18) Very recently, Trabolsi has reported a covalent organic framework containing mechanically interlocked CB[7] units.(19) Conversely, metal organic cages are discrete self-assembled structures that are soluble in organic or aqueous solution whose properties can be tailored by altering the structures of the constituent building blocks. Metal organic cages have been used for basic studies of molecular recognition processes, to tame highly reactive species (e.g. P4), as catalysts, for sensing and imaging, for drug delivery, and even as therapeutics themselves.(15a,15c,20)

Several years ago, we saw the opportunity to integrate the desirable molecular recognition properties and stimuli responsiveness of CB[n] hosts with the desirable structural features of metal organic polyhedra (MOP) to create multivalent architectures that would be particularly well suited toward (targeted) therapeutic and imaging applications. Toward this goal, we reported the synthesis of bis(pyridyl) ligand L1 and its self-assembly with Pd(NO<sub>3</sub>)<sub>2</sub> to yield the cubooctahedral Fujita type sphere A1 which is studded with 24 methyl viologen (MV) units (Scheme 1).(21) The methyl viologen units of A1 allow the primary recruitment of CB[8] to form CB[8]•MV binary complexes which can undergo subsequent ternary complex formation with a naphthol functionalized doxorubicin prodrug. The results of MTS assays showed that A1 exhibited 10-fold higher cytotoxicity toward HeLa cancer cells than an equivalent amount of doxorubicin prodrug

alone which could be traced to the enhanced cellular uptake of the larger ( $\approx$  6 nm) multivalent MOP-CB architecture. In follow up work we showed that related Fujita-type MOPs could be covalently functionalized with CB[7] and co-functionalized *via* click chemistry with dyes (e.g. fluorescein, cyanine 5.5), targeting ligands (e.g. biotin, RGD), and PEG groups.(22)



**Scheme 1.** a) Self-assembly of palladium MOP conjugated with CB[n]s. b) Self-assembly of water-soluble iron-based tetrahedra utilizing dynamic covalent coordinative bonds developed by the Nitschke group.

Despite these advances, the Fujita type systems are made using transition metals such as palladium and platinum which can be cytotoxic on their own. Furthermore, the non-covalent attachment of the CB[n] units discussed above was deemed less attractive for future *in vivo* biomedical application due to the potential for premature decomplexation. Accordingly, we envisioned that

related MOP architectures based on biocompatible metals that feature either mechanically interlocked or covalently connected CB[n] would be desirable. We were drawn to the pioneering work of Nitschke and co-workers who have developed iron-based metal organic cages that are based on subcomponent self-assembly of iron salt, aniline derivatives, and aryl aldehydes (e.g. FeSO<sub>4</sub> + **L2a** + **L2b**; Scheme 1).(23) Nitschke has created water soluble versions of these metal organic cages, demonstrated their biocompatibility, and their use in materials science (e.g. hydrogels) and for uptake and release applications.(24) Accordingly, we decided to explore a strategic merger of the structural features of iron based MOPs with the recognition properties of CB[n]. In this paper we report our work directed toward the preparation of iron based Nitschke type MOPs with mechanically interlocked CB[n] units which was envisioned to allow uptake and release of drugs within a multivalent architecture.

**Results and Discussion.** This results and discussion section is organized as follows. First, we describe the self-assembly of Nitschke-type tetrahedron 6 by the self-assembly of viologen dianiline 4 and aldehyde 5 in the presence of Fe(OTf)<sub>2</sub> and the threading of CB[7] to yield tetrahedron 7 with mechanically interlocked CB[7] units. Next, we describe the preparation of analogous viologen bipyridine ligands 11 and 16 and their self-assembly with Fe<sup>II</sup> salts in CH<sub>3</sub>CN to deliver tetrahedra 12 and 13 and cubes 17 and 18.

Synthesis of Dianiline Ligand 4 with Viologen Binding Binding Domain. In order to create a self-assembled MOP that features CB[n] binding domains according to Nitschke's subcomponent self-assembly strategy required the preparation of a linear dianiline containing a CB[n] binding

domain. For this purpose, we designed compound 4 (Scheme 2) which features a central viologen unit which was introduced to the CB[n] field by Kaifer and Kim as an excellent guest for the CB[7] and CB[8] hosts.(6,7i,7j,25) Compound 1 was prepared by reaction of 4,4-bipyridine with 2,4dinitrofluorobenzene in anhydrous CH<sub>3</sub>CN according to a literature procedure.(26) Separately, benzidine was reacted with (Boc)<sub>2</sub>O to deliver 2 as described in the literature.(27) Subsequently, 1 was heated with 2.0 equiv. 2 in refluxing EtOH overnight followed by addition of THF which caused 3 to precipitate in 96% yield; this type of reaction is referred to as the Zincke reaction.(28) Finally, the t-butoxycarbonyl groups of 3 were deprotected by treatment with CH<sub>3</sub>CO<sub>2</sub>H (TFA) in CH<sub>2</sub>Cl<sub>2</sub> to deliver 4 as its chloride salt in 98% yield. In accord with its high symmetry, Figure 2a shows the <sup>1</sup>H NMR spectrum recorded for **4** in CD<sub>3</sub>CN which shows two <sup>1</sup>H NMR resonances for the symmetry equivalent viologen protons at 9.22 and 8.64 ppm (H<sub>e</sub> and H<sub>f</sub>, respectively) and four additional resonances (H<sub>a</sub> – H<sub>d</sub>) for the phenylene spacer and terminal aniline rings. The <sup>13</sup>C NMR spectrum of 4 shows 11 resonances in the aromatic region as expected based on symmetry considerations.

$$O_2N$$
 $NO_2$ 
 $O_2N$ 
 $NO_2$ 
 $O_2N$ 
 $NO_2$ 
 $O_2N$ 
 $NO_2$ 
 $O_2N$ 
 $O_2N$ 

*Scheme 2.* Synthesis of dianiline ligand 4 as its chloride and PF<sub>6</sub> salts.

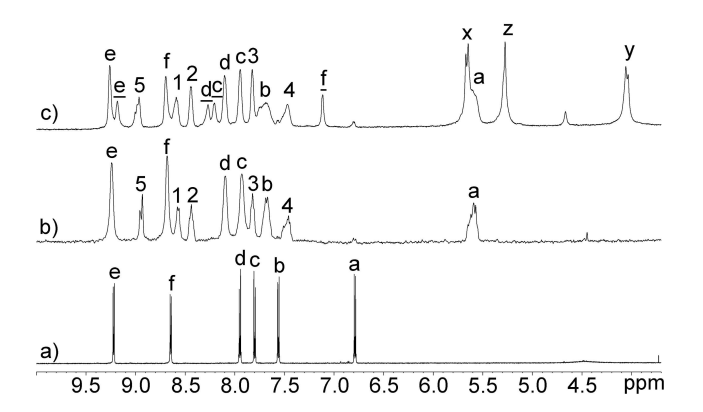
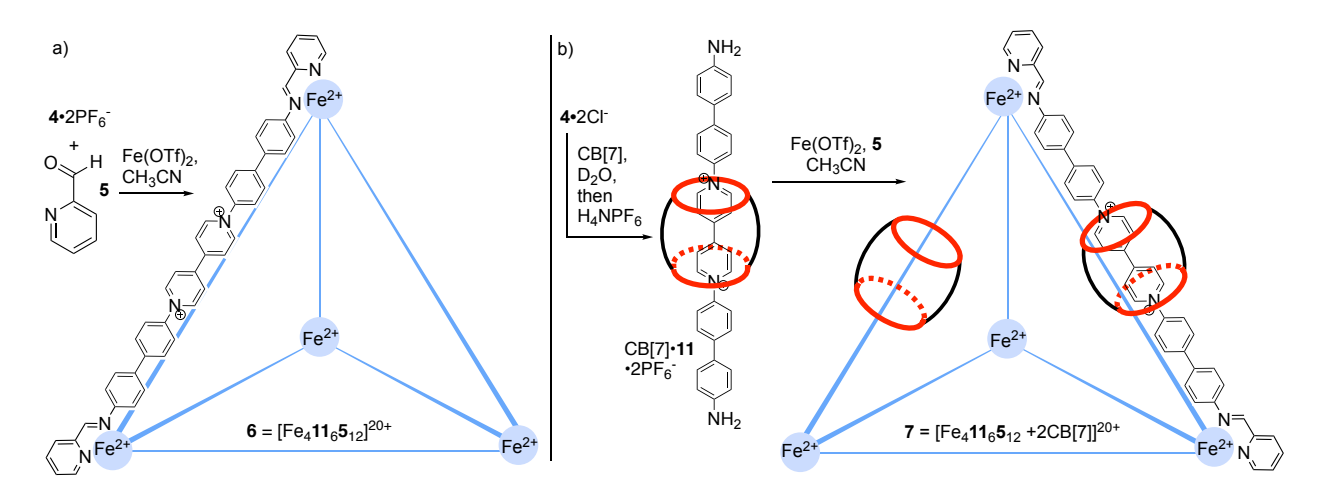


*Figure 2.* <sup>1</sup>H NMR spectra recorded (600 MHz, CD<sub>3</sub>CN, RT) for: a) **4**•2PF<sub>6</sub>, b) **6**•20PF<sub>6</sub>, and c) **7**•20PF<sub>6</sub>. The resonances marked with an underscore (\_) denote protons on ligand that contain mechanically interlocked CB[7].

Self-assembly of Nitschke-type Tetrahedron 6. With dianiline ligand 4•2Cl in hand, we sought to react it with pyridine-2-carboxyaldehyde (5) and FeSO<sub>4</sub> in water to deliver self-assembled tetrahedron 6. Unfortunately, under aqueous conditions no product was formed which in retrospect is due to the hydrolysis of the labile imine linkages.(29) Accordingly, we performed counterion exchange of 4 from the chloride salt to the PF<sub>6</sub> salt by treatment of an aqueous solution of 4 with NH<sub>4</sub>PF<sub>6</sub> to precipitate 4•2PF<sub>6</sub> (Scheme 2). Compound 4•2PF<sub>6</sub> is soluble in CH<sub>3</sub>CN. Next, we performed the self-assembly reaction of a solution of 4•2PF<sub>6</sub>, 5, and Fe(OTf)<sub>2</sub> in dry acetonitrile at 60 °C for 24 hours (Scheme 3). Upon addition of Fe(OTf)<sub>2</sub>, an immediate color change from dark brown to deep purple was observed. UV/Vis spectroscopy shows the presence of a new absorption band from 500 – 615 nm (Supporting Information, Figure S31). This dramatic color change is commonly observed during the formation of Nitschke-type cages due to the metal-to-ligand

charge-transfer interactions associated with low-spin Fe<sup>II</sup> in a hexaimine ligand environment.(30) The <sup>1</sup>H NMR spectra of tetrahedron **6** is shown in Figure 2b which displays a total of 10 aromatic CH resonances and one imine CH resonance in accord with the depicted structure. assignments of  $H_1 - H_4$  to the pyridine portion of cage 6 and  $H_a - H_f$  to the extended viologen region of cage 6 was determined by the cross peaks in the two dimensional COSY spectrum (Supporting Information, Figure S22). The resonance for H<sub>a</sub> undergoes a dramatic upfield shift (Figure 2a,b) from 6.79 ppm to 5.60 ppm which is diagnostic of self-assembly because H<sub>a</sub> is in the anisotropic shielding region of an adjacent ligand at the Fe corner. Importantly, the resonance at 8.84 ppm is characteristic of the newly formed imine bond (HC=N) group. Nitschke has shown that this resonance is particularly sensitive to the presence of diastereomers of the self-assembled tetrahedral cage.(31) Each metal ion corner of 6 can possess either the  $\Delta$  or  $\Lambda$  stereochemistry which leads to 3 possible combinations ( $\Delta\Delta\Delta\Delta$ ,  $\Delta\Delta\Delta\Lambda$ , and  $\Delta\Delta\Lambda\Lambda$ ) and their enantiomers. Figure 2b shows the presence of two peaks for H<sub>5</sub> at 8.97 and 8.94 ppm which indicates the presence of at least two diastereomeric forms of 6 are formed. Unfortunately, we were unable to obtain either an x-ray crystal structure or observe a parent ion by electrospray ionization mass spectrometry for 6. Accordingly, we turned to diffusion ordered spectroscopy (DOSY) to obtain information about the size of **6**.(32) The diffusion coefficient of **6** was measured as  $D = 3.68 \times 10^{-10} \text{ m}^2 \text{ s}^{-1}$  in  $CD_3CN$ at 298 K which is 4.7-fold lower than that measured for dianiline 4 (D =  $1.74 \times 10^{-9} \text{ m}^2 \text{ s}^{-1}$ ) under identical conditions which indicates formation of a significantly larger species. We used the Stokes-Einstein equation(32-33) to calculate the hydrodynamic diameter for 6•20PF<sub>6</sub> as 34.6 Å. We created an MMFF94s minimized molecular model of 6 and measured the distance from the centroid of the four Fe centers to the furthest point of the assembly (22.1 Å) which gives a diameter of 44.2 Å which is slightly larger than that determined by DOSY. This discrepancy may be due to the fact that the assembly is tetrahedral rather than spherical. The diffusion coefficient measured for  $\bf 6$  is slightly smaller than that measured by Nitschke for an assembly constructed from an 2,6-bis(4-aminophenyl)anthracene based ligand (D =  $3.82 \times 10^{-10} \text{ m}^2 \text{ s}^{-1}$ )(31b) which provides added support for our formulation of the tetrahedral geometry shown in Scheme 4.



**Scheme 3.** Self-assembly of Nitschke-type tetrahedron 6 and its analogue 7 with mechanically interlocked CB[7].

**Table 1.** Diffusion coefficients (m/s²) and calculated hydrodynamic diameters (Å) for the different ligands and self-assembled structures. Conditions: CD<sub>3</sub>CN, 298 K.

Compound	$D_{MeCN}(m^2/s)$	Hydrodynamic Diameter (Å)
<b>4•</b> 2PF <sub>6</sub>	$(1.74 \pm 0.01) \times 10^{-9}$	7.3
<b>4</b> •CB7•2PF <sub>6</sub>	$(5.53 \pm 0.28) \times 10^{-10}$	23.0

<b>6•</b> 20PF <sub>6</sub>	$(3.68 \pm 0.80) \times 10^{-10}$	34.6
<b>7•</b> 20PF <sub>6</sub>	$(2.71 \pm 0.07) \times 10^{-10}$	46.8
11•2PF <sub>6</sub>	$(7.30 \pm 0.39) \times 10^{-10}$	17.4
<b>11•</b> CB7•2PF <sub>6</sub>	$(5.08 \pm 0.38) \times 10^{-10}$	25.1
<b>12•</b> 20PF <sub>6</sub>	$(3.08 \pm 0.12) \times 10^{-10}$	41.4
<b>13•</b> 20PF <sub>6</sub>	$(3.06 \pm 0.15) \times 10^{-10}$	41.7
<b>16•2</b> PF <sub>6</sub>	$(7.71 \pm 0.11) \times 10^{-10}$	16.5
<b>16•</b> CB7•2PF <sub>6</sub>	$(5.66 \pm 0.34) \times 10^{-10}$	22.5
<b>17•</b> 40PF <sub>6</sub>	$(1.40 \pm 0.01) \times 10^{-10}$	91.3
<b>18•</b> 40PF <sub>6</sub>	$(1.25 \pm 0.24) \times 10^{-10}$	102

Investigation of the Complexation of Dianiline 4 with CB[n] (n = 7, 8). The ultimate goal of this project is to create a mechanically interlocked scaffold with CB[8] units on the edges of the MOP that will allow complexation of a multiplicity of drug molecules by the second binding site of CB[8] for drug delivery purposes. As a prelude to such studies, we performed separate titration experiments of dianiline ligand 4•2Cl with CB[7] and CB[8] in D<sub>2</sub>O. At a 1:1 stoichiometric ratio of 4:CB[7],  $^{1}$ H NMR spectroscopy (Supporting Information, Figure S11) shows that the resonances for H<sub>e</sub> and H<sub>f</sub> shift significantly upfield (H<sub>e</sub> from 9.48 ppm to 9.20 ppm; H<sub>f</sub> from 8.83

ppm to 7.86 ppm) compared to 4 alone. The cavity of CB[n] constitutes a magnetically shielding environment, (34) which provides strong evidence that CB[7] resides on the central viologen in the CB[7]•4 complex. As additional quantities of CB[7] is added, the <sup>1</sup>H NMR resonances for H<sub>e</sub> and H<sub>f</sub> shift back toward those observed for free 4 whereas the resonances for the terminal aniline units (H<sub>a</sub> - H<sub>d</sub>) shift upfield. At a 1:2 4:CB[7] stoichiometry a simple spectrum is observed which is indicative of a CB[7]•4•CB[7] complex where the CB[7] units reside on each terminal aniline unit. This change in binding site occurs when the free energy of CB[7] binding to two aniline units is larger than one CB[7] binding event at the central viologen unit. Subsequently, we attempted a titration experiment with CB[8] and 4. Unfortunately, at equimolar ratios, we observed the immediate formation of a precipitate.(35) The small amount of material remaining in solution appears to be the CB[8]2•42 complex based on DOSY measurements (Supporting Information, Figure S17). It is well known that CB[8] can bind two aromatic guests simultaneously.(7j,25a,36) At a 1:1 CB[8]:4 stoichiometric ratio, this opens up the possibility that CB[8] will bind two aniline termini in a head-to-tail fashion which ultimately leads to oligomerization. A 2:1 mixture of 4 and CB[8] was soluble in D<sub>2</sub>O and the <sup>1</sup>H NMR showed that the aniline termini were encapsulated inside CB[8] (Supporting Information, Figure S15). Although we were disappointed by our inability to obtain a discrete 1:1 CB[8]•4 complex we decided to move on toward the mechanical interlocking of CB[7] onto the edges of tetrahedron **6**.

Incorporation of Mechanically interlocked CB[n] onto the Edges of Assembly 6 to Create Assembly 7. Given our successful formation of the CB[7]•4 complex where the central viologen binding domain is complexed, we turned our efforts toward mechanically interlocking CB[7] on the edges of 6 (Scheme 3b). Initially, we tried to perform the one-pot self-assembly of a 6:12:4:6

mixture of 4•2Cl, 5, FeSO<sub>4</sub>, and CB[7] in water but were unsuccessful. Based on the precedent of Nitschke,(29) we also explored the addition of K<sub>2</sub>SO<sub>4</sub> to increase ligand solubility and product stability and separately tested Fe(OTf)<sub>2</sub> as the iron source, but were uniformly unable to detect any self-assembled tetrahedral assembly. We surmise that the product is hydrolytically unstable under aqueous conditions, or that the iron salt may preferentially interact with the portals of CB[7] which disfavors the desired assembly pathway. Accordingly, we decided to perform the self-assembly process in CH<sub>3</sub>CN as was successful for 6. First, we created the discrete 1:1 CB[7]•4 complex by mixing equimolar amounts of CB[7] and 4.2Cl in water, followed by the addition of excess NH<sub>4</sub>PF<sub>6</sub> or LiNTf<sub>2</sub> which causes the precipitation of the CB[7]•4•2PF<sub>6</sub> or CB[7]•4•2NTf<sub>2</sub> salts. The use of counterion exchange to solubilize CB[7] complexes in organic solution was first reported by Kaifer.(25d) CB[7]•4•2PF<sub>6</sub> and CB[7]•4•2NTf<sub>2</sub> are soluble in CH<sub>3</sub>CN and DMSO. Subsequently, self-assembly of a 6:12:4 mixture of CB[7]•4•2PF<sub>6</sub> salt, 5, and Fe(OTf)<sub>2</sub> was performed in dry acetonitrile at 60 °C for 24 hours. The <sup>1</sup>H NMR spectrum recorded in CD<sub>3</sub>CN (Figure 2c) shows two sets of peaks for each of the viologen protons (He, Hf) and each of the aniline protons (H<sub>c</sub>, H<sub>d</sub>) in a 1.95:1 ratio as determined by integration. Of particular note is that  $\underline{H_f}$  is upfield shifted by 1.57 ppm to 7.11 ppm whereas  $\underline{H_c}$  and  $\underline{H_d}$  are slightly downfield shifted ( $\approx$ 0.2-0.3 ppm) within assembly 7•20PF<sub>6</sub> relative to assembly 6•20PF<sub>6</sub>. These changes in chemical shift are comparable to that observed during the formation of the CB[7]•4 complex which is strong evidence for the mechanical interlocking of an average of 1.95 CB[7] molecules onto the cage 6 to give the depicted structure of cage 7. Conversely, the major resonances for H<sub>f</sub>, H<sub>c</sub>, and H<sub>d</sub> in 7 for the uncomplexed edges appear at chemical shifts that are comparable to that observed for 6. Approximately two edges of 7 are complexed with CB[7] and four edges remain uncomplexed.

The DOSY spectrum of 7•20PF<sub>6</sub> shows the presence of a single species with a diffusion coefficient  $(D = 2.71 \times 10^{-10} \text{ m}^2 \text{ s}^{-1})$  with a diameter of 46.8 Å calculated according to the Stokes-Einstein The calculated diameter of 7 is 12.2 Å larger than that of 6.20PF<sub>6</sub> which is approximately twice the radius of CB[7] (8.0 Å).(5a,6) Unfortunately, we were unable to obtain ESI-MS data for assembly 7. We observe the precipitation of CB[7] during the self assembly of cage 7 which establishes that CB[7] can decomplex from CB[7]•4 complex during the reaction. Related experiments conducted with lower amounts of CB[7] (e.g. three free 4 and three CB[7]•4), still lead to assembly 7. Attempts to prepare 7 by a slippage(37) process involving heating 6 and CB[7] in CD<sub>3</sub>CN (60 °C) were unsuccessful due to the insolubility of CB[7]. Having successfully mechanically interlocked least 2 CB[7] molecules onto the edges to create 7 we tested the stability of 7 in water as a precursor step to the envisioned use of these assemblies in drug delivery. When water was added to either assembly 6 or 7, we observed the disappearance of the characteristic purple color and the <sup>1</sup>H NMR displayed resonances for the starting materials 4 and 5. In particular, the loss of the imine H<sub>5</sub> peak and the emergence of the aldehyde O=C-H resonance provide strong evidence that the cage underwent hydrolysis in water due to hydrolytic instability. Given this finding it appeared that the envisioned mechanical interlocking of CB[n] onto the edges of Nitschke-type assemblies was a dead end which prompted us to explore ligands whose assemblies would be stable in water.

Synthesis of Bipyridine Based Viologen Ligand 11 and its Self Assembly to give MOP 12. To circumvent the problems with the aqueous hydrolysis of the imine bonds that hold assembly 7 together, we redesigned our system using a more robust ligand that is not prepared in a

subcomponent self-assembly process. We settled on ligand 11 which features 2,2'-bipyridine termini as ligands and a central viologen unit as the CB[n] binding domain (Scheme 4). First, we performed the Suzuki reaction between commercially available starting materials 8 and 9 using Pd(Ph<sub>3</sub>)<sub>4</sub> as catalyst to deliver 10 in 92% yield.(38) Next, we allowed aniline 10 to react with 1 by a double Zincke reaction in refluxing EtOH to deliver target ligand 11.2Cl in 97% yield. Compound 11 was fully characterized spectroscopically (<sup>1</sup>H, <sup>13</sup>C, ESI-MS). For example, the <sup>1</sup>H NMR spectrum of 11 recorded in D<sub>2</sub>O (Supporting Information, Figure S32) show the characteristic viologen protons (H<sub>i</sub> and H<sub>k</sub>) resonances at 9.50 ppm and 8.83 ppm, a pair of coupled doublets for the phenylene linker (H<sub>i</sub> and H<sub>h</sub>) at 8.14 ppm and 8.00 ppm, and the expected seven additional aromatic resonances (H<sub>a</sub> - H<sub>g</sub>) for the 2,2'-bipyridyl end groups (two triplets (H<sub>a</sub> and H<sub>b</sub>), a singlet (H<sub>g</sub>), and three pairs of doublets (H<sub>d</sub> - H<sub>f</sub>)). In the <sup>13</sup>C NMR spectrum, all 17 resonances expected for 11 on the basis of its depicted  $C_{2\nu}$ -symmetric structure were observed experimentally. Compound 11•2Cl could be transformed into the corresponding PF<sub>6</sub> or NTf<sub>2</sub> salts by treatment of aqueous solutions of 11.2Cl with an excess of NH<sub>4</sub>PF<sub>6</sub> or LiNTf<sub>2</sub> which resulted in precipitation of 11•2PF<sub>6</sub> and 11•2NTf<sub>2</sub> which are used in some of the self-assembly reactions described below.

**Scheme 4.** Synthesis of modified bipyridyl ligand 11.

Before proceeding to the self-assembly of 11•2Cl we decided to test its complexation with CB[7] and separately with CB[8] in the absence of iron salts. Simple <sup>1</sup>H NMR spectroscopic titration shows that 11•2Cl binds to CB[7] in D<sub>2</sub>O (Supporting Information, Figure S42). At a 1:0.9 ratio of 11:CB[7], we observe upfield changes in chemical shift for viologen protons H<sub>i</sub> and H<sub>k</sub> as well as phenylene protons  $H_h$  and  $H_i$  whereas the resonances for  $H_c$  and  $H_g$  which are on the 2,2bipyridine end groups do not experience significant changes in chemical shift. This indicates that the CB[7] units in the CB[7]•11 complex are not at a fixed location but rather shuttle between the phenylene and viologen binding sites. At a 1:2 11:CB[7] ratio, the resonances for the phenylene linker H<sub>h</sub> and H<sub>i</sub> undergo further upfield changes in chemical shift as the CB[7] units become localized on the phenylene binding sites to accommodate the presence of two molecules of CB[7]. Somewhat differently, the <sup>1</sup>H NMR spectrum of a 1:1 mixture of 11 and CB[8] (Supporting Information, Figure S46 and S47) shows only small shifting for the viologen protons H<sub>i</sub> and H<sub>k</sub> (H<sub>i</sub> from 9.50 to 9.40 ppm, H<sub>k</sub> from 8.83 to 8.96 ppm) whereas the phenylene protons undergo more substantial upfield shifts (H<sub>h</sub> from 8.00 to 7.36 ppm; H<sub>i</sub> from 8.14 to 7.60 ppm) upon complexation.

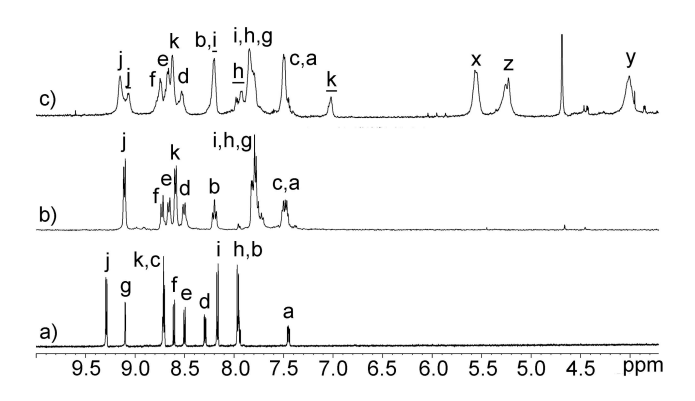


*Figure 3.* <sup>1</sup>H NMR spectra recorded (600 MHz, CD<sub>3</sub>CN, RT) for: a) **11•**2PF<sub>6</sub>, b) **12•**20NTf<sub>2</sub>, and c) **13•**20PF<sub>6</sub>. The resonances marked with an underscore (\_) denote protons on ligand that contain mechanically interlocked CB[7].

Encouraged by the ability to observe 1:1 complexation between 11 and CB[7] or CB[8], we moved on to the self-assembly studies. Initially, we performed the self-assembly of 11•2PF<sub>6</sub> and Fe(OTf)<sub>2</sub> (6:4 molar ratio) in CH<sub>3</sub>CN at 60 °C for 24 hours which delivers self-assembled tetrahedron 12.20PF<sub>6</sub> (Scheme 5). Immediately after mixing, we observed a color change from yellow-brown to red which is characteristic of the formation of the iron-bipyridine complex. Figure 3a,b shows the <sup>1</sup>H NMR spectra recorded for 11•2PF<sub>6</sub> and for the self-assembled MOP 12•20NTf<sub>2</sub>. Upon selfassembly, the resonances for  $H_c$  and  $H_g$  which are adjacent to the bipyridine N-atoms undergo significant upfield shifts (H<sub>c</sub>: 8.71 ppm to 7.50 ppm; H<sub>g</sub>: 9.10 ppm to 7.79 ppm) which reflects that these protons feel the anisotropic shielding effect of an adjacent bipyridine when complexed to the metal center.(39) Conversely, H<sub>a</sub>, H<sub>d</sub>, H<sub>e</sub>, and H<sub>f</sub> undergo slight downfield shifts upon selfassembly (H<sub>a</sub>: 7.94 to 8.20 ppm, H<sub>d</sub>: 8.29 to 8.50 ppm, H<sub>e</sub>: 8.50 to 8.65 ppm, and H<sub>f</sub>: 8.61 to 8.72 ppm) likely due to changes in the electronics of the bipyridine ring upon coordination to iron. In this case, the observation of a single set of sharp <sup>1</sup>H and <sup>13</sup>C NMR (Supporting Information, Figure S50) resonances of the expected number and multiplicity strongly suggests the formation of a single diastereomer of 12 which we formulate as the racemic mixture of  $\Delta\Delta\Delta\Delta$ -12 and  $\Delta\Delta\Delta\Lambda$ -12. The UV/Vis spectra recorded for 11 and assembly 12 in CH<sub>3</sub>CN is given in the Supporting Information (Supporting Information, Figure S70). The spectra for 12 shows a new band with  $\lambda_{max}$ = 539 nm which is due to metal to ligand charge transfer upon complexation, (39b, 40) as well as the shifting of a shorter wavelength  $\lambda_{max}$  from 294 (for 11) to 315 nm (for 12). We used DOSY

NMR to determine the diffusion coefficient for  $12 \cdot 20PF_6$  in acetonitrile at 25 °C (D =  $3.08 \times 10^{-10}$  m<sup>2</sup> s<sup>-1</sup>) as given in Table 1 which is 2.4-fold slower than the free ligand  $11 \cdot 2PF_6$  (D =  $7.30 \times 10^{-10}$  m/s<sup>2</sup>) which provides support for self-assembly. The calculated hydrodynamic diameter of  $12 \cdot 20PF_6$  is 41.4 Å which is somewhat larger than Nitschke-type cage  $6 \cdot 20PF_6$  (34.6 Å).(41) Finally, Figure 4a shows the electrospray ionization mass spectrum recorded for assembly 12 as its PF<sub>6</sub> salt. We observe the presence of ions in the mass spectrum that correspond to the 6+ to 9+ ions of  $12 \cdot 20PF_6$  ([Fe<sub>4</sub>11<sub>6</sub> +14(PF<sub>6</sub>)]<sup>6+</sup> m/z = 994.23; [Fe<sub>4</sub>11<sub>6</sub> +13(PF<sub>6</sub>)]<sup>7+</sup> m/z = 831.35; [Fe<sub>4</sub>11<sub>6</sub> +12(PF<sub>6</sub>)]<sup>8+</sup> m/z = 709.30; [Fe<sub>4</sub>11<sub>6</sub> +11(PF<sub>6</sub>)]<sup>9+</sup> m/z = 614.38) upon successive loses of PF<sub>6</sub> counterions. The  $12 \cdot 20PF_6$  salt could be transformed to the  $12 \cdot 10SO_4$  salt by treatment of a CH<sub>3</sub>CN solution with excess K<sub>2</sub>SO<sub>4</sub> which gave the sulfate salt as a solid precipitate. MOP  $12 \cdot 10SO_4$  was soluble in water and did not undergo any change by <sup>1</sup>H NMR upon standing at 25 °C for > 2 weeks. MOP  $12 \cdot 10SO_4$  could also be synthesized directly under aqueous conditions from a 6:60:4 mixture of  $11 \cdot 2C1$ , K<sub>2</sub>SO<sub>4</sub>, and FeSO<sub>4</sub> by sonicating for 30 minutes at room temperature and then heating at 60 °C for 24 hours (Scheme 5, Figure S57).

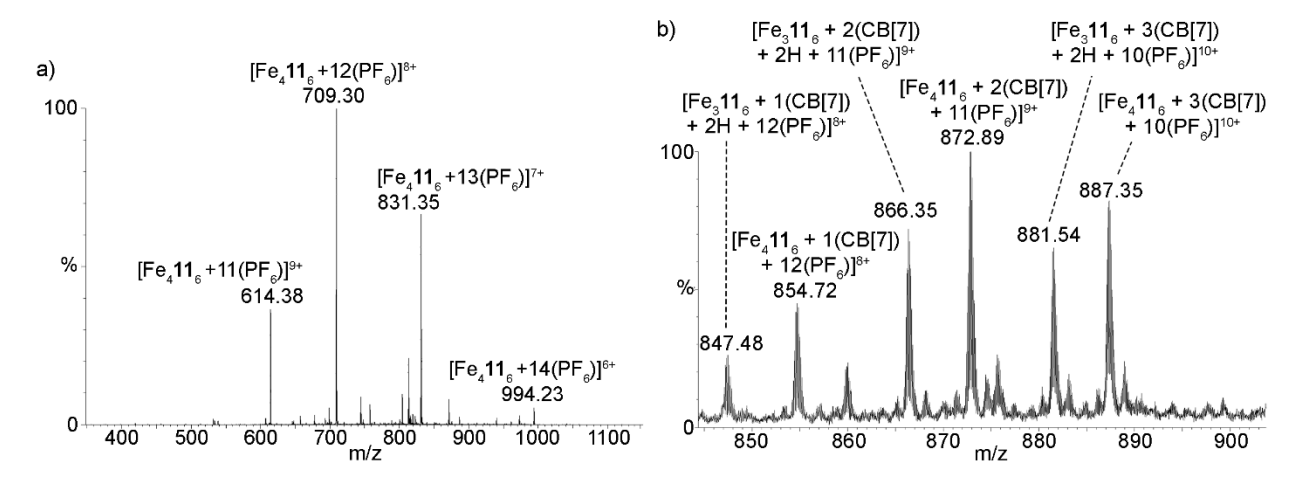
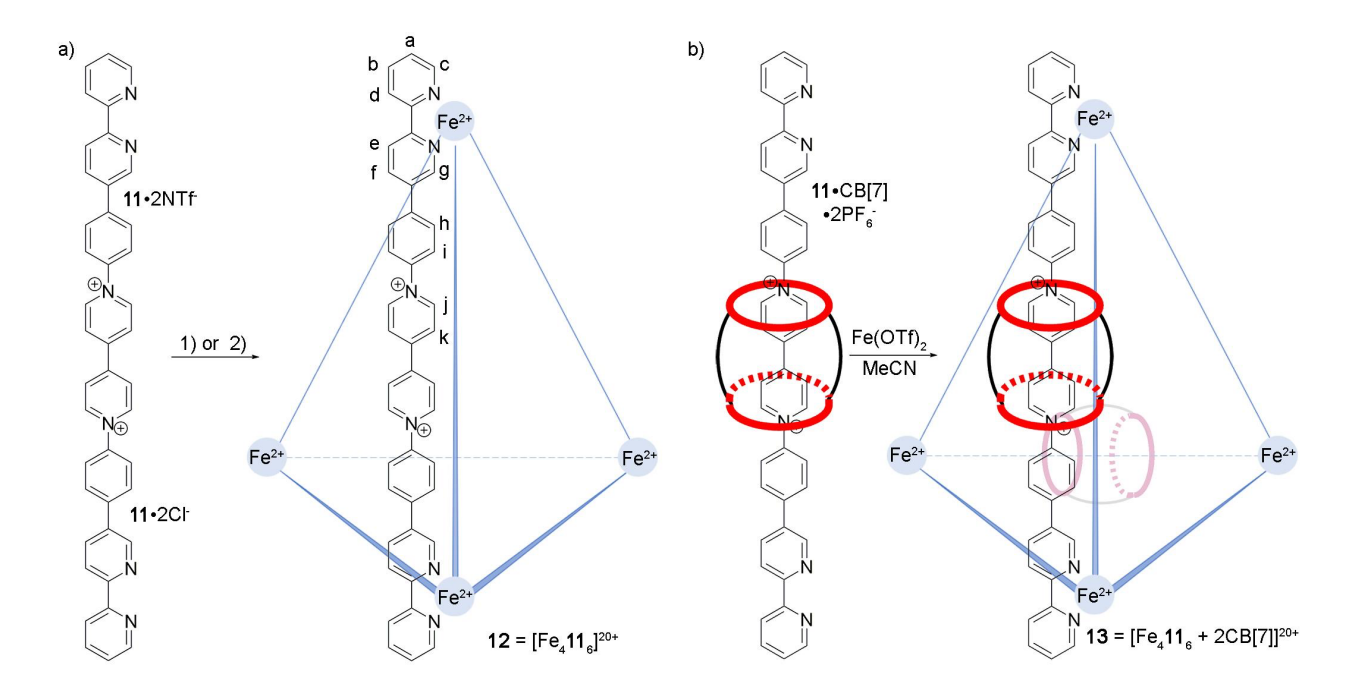


Figure 4. Mass spectra recorded for CH<sub>3</sub>CN:DMSO solutions of: a) 12•20PF<sub>6</sub>, and b) 13•20PF<sub>6</sub>.



**Scheme 5.** Self-assembly of: a) tetrahedron **12** performed in either CH<sub>3</sub>CN or H<sub>2</sub>O, and b) tetrahedron **13** which incorporates CB[7] units. Conditions: 1) Fe(NTf<sub>2</sub>)<sub>2</sub>, CH<sub>3</sub>CN, 60 °C, 2) K<sub>2</sub>SO<sub>4</sub>, FeSO<sub>4</sub>, 60 °C.

Mechanical Interlocking of CB[n] onto the Edges of Cage 12 to Give Cage 13. Encouraged by the successful self-assembly of 12 under aqueous conditions, we decided to target the incorporation of mechanically interlocked CB[n] components. For this purpose, we performed the self-assembly of 11•2Cl, CB[7], K<sub>2</sub>SO<sub>4</sub>, FeSO<sub>4</sub> (6:6:60:4) in water (60 °C) for 24 hours. The reaction mixture did not change color over this time period as was expected and remained heterogenous throughout. Furthermore, we did not observe upfield shifting for H<sub>c</sub> and H<sub>g</sub> in the <sup>1</sup>H NMR spectrum which would be expected upon formation of the iron(bipyridine)<sub>3</sub> corners. Our interpretation is that the conformation heterogeneity of the 11•CB[7] complex in water (e.g. mainly on the phenylene rather than the viologen binding site hinders formation of the targeted self-

assembled cage perhaps by promoting protonation of the bipyridine units. In contrast, the <sup>1</sup>H NMR spectrum recorded in acetonitrile for the CB[7]•11•2PF<sub>6</sub> complex that had been prepared in water shows a substantial upfield shift for viologen resonance H<sub>k</sub> from 8.71 ppm for free 11•2PF<sub>6</sub> to 7.17 ppm as part of the CB[7]•11•2PF<sub>6</sub> complex which provides clear evidence for the CB[7] residing on the viologen unit (Supporting Information, Figure S43). Proton H<sub>i</sub> also undergoes a small upfield shift upon complexation whereas the remaining protons on ligand 11 undergo small downfield changes in chemical shift. Accordingly, we next performed the self-assembly of a mixture of CB[7]•11•2PF<sub>6</sub> and Fe(OTf)<sub>2</sub> in acetonitrile at 60 °C for 24 hours (Scheme 5b). The self-assembly process is also successful when CB[7]•11•2NTf<sub>2</sub> and Fe(NTf<sub>2</sub>)<sub>2</sub> are employed. The reaction mixture rapidly changes color from yellow to ruby red. MOP 13•20PF<sub>6</sub> was isolated after precipitation from the reaction mixture by the addition of Et<sub>2</sub>O followed by centrifugation, decanting the supernatant, and drying. The <sup>1</sup>H NMR of 13•20PF<sub>6</sub> recorded in CD<sub>3</sub>CN is shown in Figure 3c. The assignment of the resonances is based upon the correlations observed in the COSY spectrum (Supporting Information, Figure S65). Most strikingly, the resonance for viologen proton H<sub>k</sub> in 13 shifts dramatically upfield to 7.02 ppm compared to that observed for 12 (8.59 ppm, Figure 2b) which lacks CB[7] units. Furthermore, we observe two sets of resonances for protons H<sub>h</sub>, H<sub>i</sub>, H<sub>i</sub>, and H<sub>k</sub> of unequal (1.80 by integration) ratio by <sup>1</sup>H NMR. This <sup>1</sup>H NMR data suggests that on average four 11 ligands that are part of assembly 13 do not have mechanically interlocked CB[7] units whereas two ligands of 11 possess a mechanically interlocked CB[7] unit. Integration of the resonances for the CB[7] unit  $(H_x, H_y, H_z)$  versus the ligand protons  $(H_i \text{ and } \underline{H}_i)$ combined) also shows that 1.80 CB[7] are mechanically interlocked on 13. The slight upfield shift observed for  $\underline{H}_i$  (9.10 to 9.06 ppm) and the slight downfield shifts observed for  $\underline{H}_h$  (7.80 to 7.97

ppm) and  $\underline{H}_i$  (7.80 to 8.20 ppm) relative to  $H_i$ ,  $H_h$ , and  $H_i$  support the notion that the CB[7] units reside on the viologen binding domain in assembly 13. To gauge the size of assembly 13. 20PF<sub>6</sub> we performed DOSY NMR which allowed us to calculate the diffusion coefficient (D =  $3.06 \times 10^{-1}$ <sup>10</sup> m/s<sup>2</sup>) and the hydrodynamic diameter of assembly **13** (41.7 Å) in acetonitrile. The resonances for ligand 11 and CB[7] within assembly 13 diffuse at the same rate which provides further evidence for the interlocked nature of 13. The diffusion coefficient and hydrodynamic radius of 13 are very similar to those measured for the Nitschke-type assembly 7 which also contains interlocked CB[7] units (Table 1). Figure 4b shows a region of ESI mass spectrum obtained for 13 as its PF<sub>6</sub> salt. We observe dominant ions at m/z 887.35 ([Fe<sub>4</sub>11<sub>6</sub> + 3(CB[7]) + 10(PF<sub>6</sub>)]<sup>10+</sup>),  $872.89 ([Fe_411_6 + 2(CB[7]) + 11(PF_6)]^{9+}), \text{ and } 854.72 ([Fe_411_6 + 1(CB[7]) + 12(PF_6)]^{8+}) \text{ which}$ correspond to cage 13 with three, two, and one interlocked CB[7], respectively, as their 10+, 9+, and 8+ ions (Supporting Information, Figures S67 – S69). The combined inference of the <sup>1</sup>H NMR, DOSY, and ESI-MS data provides strong support for the formulation of 13 as a tetrahedral cage that possesses an average of 1.80, but a range of 1–3, mechanically interlocked CB[7] units. We also attempted the self-assembly of 11.2Cl, FeSO<sub>4</sub>, K<sub>2</sub>SO<sub>4</sub>, and CB[8] in water at 60 °C, but we did not observe any color change which is strong evidence against the formation of iron(bipyridine)<sub>3</sub> complexes under these conditions. We suspect that the ureidyl C=O groups of CB[8] scavenge the FeSO<sub>4</sub> and prevent assembly. Attempts to prepare the organic soluble CB[8]•11•2PF<sub>6</sub> complex were not successful according to <sup>1</sup>H NMR analysis.

Molecular Modelling of Self-Assembled Tetrahedra 12 and 13. We performed molecular modelling of tetrahedra 12 and its analogue fully interlocked with six CB[7] rings 12•CB[7]<sub>6</sub>.

Figure 5a,b shows the structures of 12 and 12 CB[7]<sub>6</sub> minimized by molecular mechanics using the MMFF94s force field implemented within the Spartan '16 software package. As can be seen, 12 features a roughly tetrahedral geometry with a large central cavity. The average distance between Fe atoms of MOP 12 is 24.9 Å and the distance from the centroid of the four Fe atoms to the outside edge of the MOP is 19.1 Å. Accordingly, the rough diameter of the MMFF94s minimized structure of 12 is 38.2 Å which is slightly smaller than the hydrodynamic diameter (41.4 Å) calculated from the DOSY data. The hydrodynamic diameter of 12 in solution also reflects the contributions of the 20 PF<sub>6</sub> counterions so this small difference is not surprising. It should be noted that the edges of 12 are slightly bowed outward in the molecular model which is likely due to electrostatic repulsion between dicationic viologen units in the overall 20+ assembly. Figure 5b shows the MMFF94s minimized structure of 12 • CB[7]<sub>6</sub> which is roughly tetrahedral with average iron-iron distances of 25.0 Å and centroid to iron distance of 15.3 Å. The structure calculated structure easily accommodates six CB[7] units and there is no evidence of close contacts or even van der Waals interactions between CB[7] units in the minimized structure of 12 • CB[7]<sub>6</sub>. Accordingly, the experimental observation that assembly 13 contains 1.8 CB[7] units on average must be due to other factors including the poor solubility of CB[7] in the reaction mixture and the potential for repulsive electrostatic interactions between the electrostatically negative convex outer surfaces of CB[7] units.(6) The distance between the centroid of the iron atoms of 12 • CB[7]<sub>6</sub> and the outer edge of the ligands is 19.3 Å which corresponds to a calculated diameter of 38.6 Å. This calculated value for 12•CB[7]<sub>6</sub> is very similar to the value measured for 13•20PF<sub>6</sub> by DOSY (Table 1).

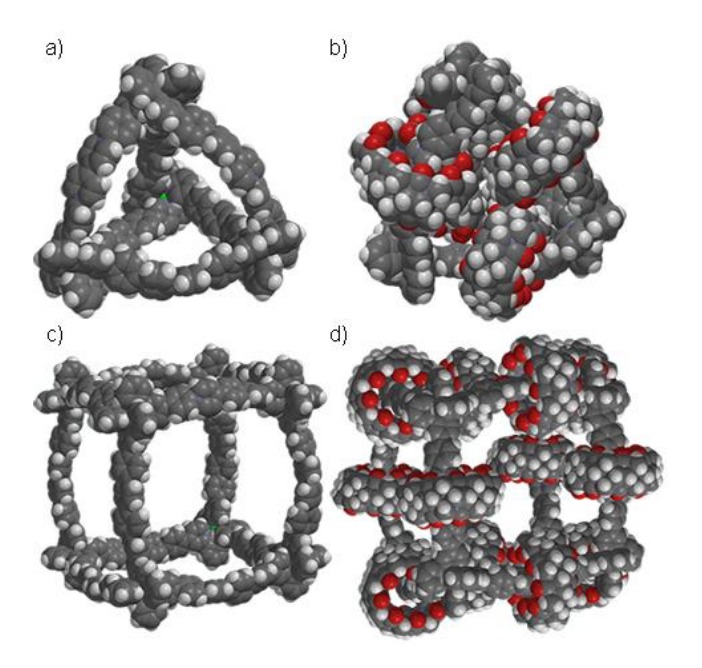


Figure 5. a) Molecular modelling of a) 12, b) 12.6CB[7], c) 17, and d) 17.12CB[7].

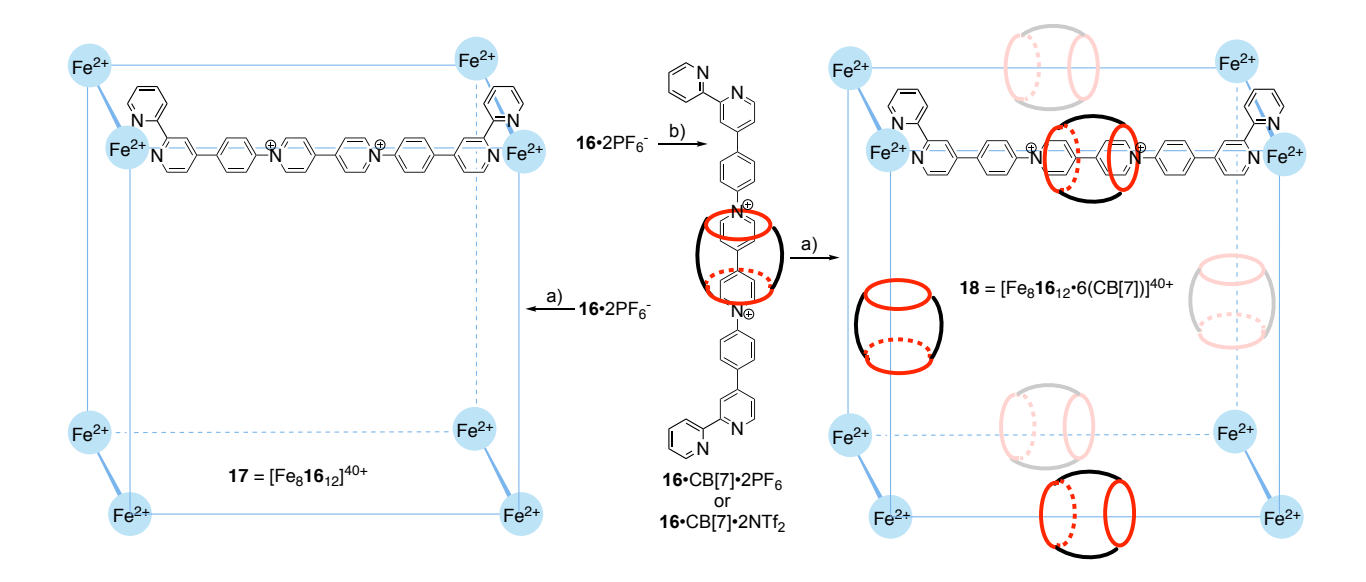
Synthesis of Isomeric Bipyridine Ligand 16 and Self-Assembly to Give Cubic MOP 17. Although we were pleased that cage 12 could be threaded to give cage 13 containing an average of two CB[7] units, we were disappointed that full occupancy of the edges (e.g. six CB[7]) could not be achieved. We decided to create a larger self-assembly that would have a larger central cavity that might be able to better accommodate a larger number of CB[n] rings. We realized that ligand 16 (Scheme 6) – which is a constitutional isomer of 11 – possesses a geometry(42) that should deliver a self-assembled cube upon reaction with Fe(II) salts. For the synthesis of 16, we first performed the Suzuki coupling reaction between commercially available 4-bromo-2,2'-bipyridine 14 and 9 using Pd(PPh<sub>3</sub>)<sub>4</sub> as catalyst to deliver 15 in 64% yield. Subsequently, the Zincke reaction(28) between 15 and 1 was performed in refluxing EtOH to deliver 16 in 77% yield. Compound 16 was fully characterized by the standard spectroscopic methods. For example, characteristic <sup>1</sup>H

NMR resonances for the viologen aromatic protons ( $H_j$  and  $H_k$ ) appear at 9.52 ppm and 8.86 ppm (Supporting Information, Figure S71) whereas a pair of aromatic doublets appear at 8.23 ppm and 8.04 ppm for the phenylene linker ( $H_i$  and  $H_h$ ) along with seven additional aromatic resonances ( $H_a - H_g$ ) are for the bipyridyl end group (triplets for  $H_a$  and  $H_b$ , a singlet for  $H_g$ , and three doublets for  $H_d - H_f$ . The <sup>13</sup>C NMR spectrum for **16** recorded in DMSO-d<sub>6</sub> (Supporting Information, Figure S72) displays 17 resonances in the aromatic region of the spectrum which is consistent with the  $C_{2\nu}$ -symmetric structure depicted in Scheme 6.

Scheme 6. Synthesis of isomeric bipyridine ligand 16.

Given our previous success in the self-assembly of 12 in acetonitrile, we first converted 16 into the corresponding organic soluble PF<sub>6</sub> and NTf<sub>2</sub> salts. To prepare self-assembled cube 17 we heated a 12:8 mixture of 16•2PF<sub>6</sub> (or 16•2NTf<sub>2</sub>) with Fe(OTf)<sub>2</sub> (or Fe(NTf<sub>2</sub>)<sub>2</sub>) in acetonitrile at 60 °C for 24 hours (Scheme 7). During the course of the reaction the color changes from orange-brown to deep purple. The UV/Vis spectra recorded for 16 and 17 is given in the Supporting Information (Figure S94). The spectrum for 17 shows a new  $\lambda_{max}$  at 544 nm which is comparable to that observed for 12 ( $\lambda_{max}$  = 539 nm) which provides strong support for the formation of the iron(bipyridine)<sub>3</sub> corners. The <sup>1</sup>H NMR spectrum recorded for 17 in CD<sub>3</sub>CN is shown in Figure

6. The assignments of the resonances to specific protons in Figure 6 are based on the correlations observed in the COSY spectrum of 17 (Supporting Information, Figure S88). Most significantly, the protons adjacent to the bipyridine N-atoms undergo substantial upfield changes in chemical shift upon transformation of 16 to 17 (H<sub>c</sub>: 8.83 to 7.62 ppm; H<sub>g</sub>: 8.73 to 7.53 ppm). These large upfield shifts reflect the fact that these protons are located in the anisotropic shielding region of the adjacent bipyridine within assembly 17 as was also seen for 12. Bipyridine protons H<sub>b</sub> (7.96 to 8.24 ppm), H<sub>d</sub> (8.51 to 8.84 ppm), and H<sub>e</sub> (8.70 to 8.96 ppm) undergo slight downfield shifts upon formation of 17 which is reflective of the change in electronics of the bipyridine ring upon coordination to Fe<sup>II</sup>. To gain insight into the size of assembly 17 we performed DOSY NMR in CD<sub>3</sub>CN at 298 K that allowed us to calculate the diffusion coefficient for 17 (D =  $1.40 \times 10^{-10}$ m/s<sup>2</sup>) and its hydrodynamic diameter (91.3 Å). Cage 17 diffuses 5.51 times slower than ligand 16 (D =  $7.71 \times 10^{-10} \text{ m/s}^2$ ) and 2.20 times slower than tetrahedron 12. Figure 5c shows the structure of an MMFF94S minimized model of 17 which is roughly cubic with an edge length of 27.7 Å. The maximum distance from the centroid of the eight iron atoms to the outer edges of 17 is 28.1 Å which corresponds to a diameter of 56.2 Å. The calculated diameter of 17 and the hydrodynamic diameter of 17 measured in solution differ in part because of the influence of the 40 PF<sub>6</sub> counterions and perhaps also due to the effects of aggregation.(32) Overall, the confluence of the data provides significant evidence for the formulation of the structure of 17 as a cubic assembly. Unfortunately, despite numerous attempts we were not able to observe ions in the ESI-MS spectrum for either 17•40PF<sub>6</sub> or 17•40NTf<sub>2</sub> that could be assigned to the depicted cubic assembly.



*Scheme 7.* Self-assembly of MOPs **17** and **18**. Conditions: a) Fe(OTf)<sub>2</sub>, CH<sub>3</sub>CN, b) D<sub>2</sub>O, CB[7], then NH<sub>4</sub>PF<sub>6</sub>.

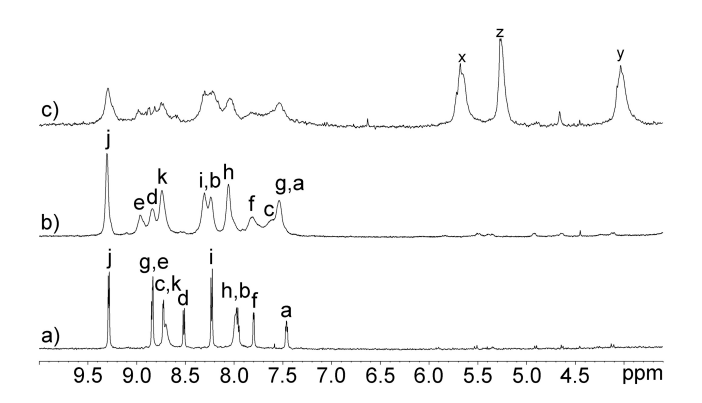


*Figure 6.* <sup>1</sup>H NMR spectra recorded (600 MHz, CD<sub>3</sub>CN, RT) for: a) **16•**2PF<sub>6</sub>, b) **17•**20PF<sub>6</sub>, and c) **18•**40NTf<sub>2</sub>.

Mechanical Interlocking of CB[7] onto the Edges of Cage 17 to Give Cage 18. Next, we set out to mechanically interlock CB[7] units onto the edges of self-assembled cube 17. Initially, we tested the complexation of an equimolar mixture of CB[7] with 16•2Cl in D<sub>2</sub>O by <sup>1</sup>H NMR (Supporting Information, Figure S79). We observe upfield shifting for phenylene protons H<sub>h</sub> (8.05)

to 7.14 ppm) and H<sub>i</sub> (8.25 to 7.34 ppm) and viologen proton H<sub>i</sub> (9.53 to 9.10 ppm) and downfield shifting of viologen proton H<sub>k</sub> (8.88 to 8.98 ppm) upon complexation with CB[7]. This data indicates that the primary binding site is the phenylene unit. Accordingly, we decided to follow the strategy employed for the assembly of 13 involving CH<sub>3</sub>CN soluble salts. Experimentally, we treated aqueous solutions of CB[7]•16•2Cl with excess LiNTf<sub>2</sub> and separately with excess NH<sub>4</sub>PF<sub>6</sub> which gave CB[7]•16•2NTf<sub>2</sub> and CB[7]•16•2PF<sub>6</sub> as precipitates that could be isolated by centrifugation, washing with water, and drying under high vacuum (Scheme 7). For the selfassembly reaction, we heated equimolar mixtures of CB[7]•16•2NTf<sub>2</sub> (or CB[7]•16•2PF<sub>6</sub>) and Fe(NTf<sub>2</sub>)<sub>2</sub> (or Fe(OTf)<sub>2</sub>) at 60 °C in acetonitrile for 24 hours to give 18. The reaction mixture rapidly assumes a deep purple color. Assembly 18 can be isolated by precipitation from the reaction mixture by addition of Et<sub>2</sub>O followed by centrifugation, decantation, and drying. Figure 6c shows the <sup>1</sup>H NMR spectrum recorded for **18** in CD<sub>3</sub>CN which is broadened and unfortunately the multiplicity cannot be observed for individual resonances. The broadness of the <sup>1</sup>H NMR spectrum rendered the COSY spectrum of no value. However, a comparison of the aromatic regions of Figures 6b and 6c make it clear that very similar assemblies are formed in both cases. Furthermore, integration of the resonances for the CB[7] units (H<sub>x</sub>, H<sub>y</sub>, H<sub>z</sub>) versus those of ligand 16 allow us to determine that assembly 18 contains an average of 6.59 molecules of CB[7]. We acquired the DOSY spectrum for 18 in acetonitrile which established that the CB[7] units of the assembly diffuse at the same rate as aromatic units of the assembly which provides strong evidence for the mechanical interlocking of the CB[7] units onto the edges of the assembly. Figure 5d shows an MMFF94s minimized model of 17•(CB[7])12 which does not show any steric interactions between the adjacent CB[7] units. The observation that assembly 18 contains an average of 6.59

CB[7] units must be due to other factors including the poor solubility of CB[7] in the reaction medium or perhaps unfavorable electrostatic interactions between the electrostatically positive convex faces of the CB[7] units. The DOSY spectrum allowed us to calculate the diffusion coefficient for 18 (D =  $1.25 \times 10^{-10}$  m/s²) along with its hydrodynamic diameter (102 Å). The hydrodynamic diameter of 18 is very similar to that of 17 (91.3 Å) which provides further support for the formulation of both 17 and 18 as cubes. Overall, the data provides clear evidence for the incorporation of multiple CB[7] units onto the edges of assembly 18 but, unfortunately, even with this larger cubic system it was not possible to achieve full occupation of all 12 edges with CB[7] units.

Conclusions. In summary, we have reported our initial investigations into the preparation of MOPs that contain mechanically interlocked CB[n] units as a precursor to using the molecular recognition properties of such assemblies for drug delivery purposes. Initially, we prepared dianiline ligand 4•2Cl – which contains a central viologen unit as a CB[n] binding site – and performed self-assembly with pyridine-2-carboxaldehyde and Fe(OTf)<sub>2</sub> in acetonitrile and observed the formation of a single species by <sup>1</sup>H and DOSY NMR that we assign as tetrahedron 6. When the organic soluble CB[7]•11•2PF<sub>6</sub> complex was self-assembled with Fe(OTf)<sub>2</sub> in acetonitrile, assembly 7 with an average of 1.95 mechanically interlocked CB[7] units was obtained. Unfortunately, MOPs 6 and 7 were hydrolytically unstable in water and therefore are not appropriate for drug delivery studies. Accordingly, analogous organic soluble ligands 11•2(NTf<sub>2</sub>) and 16•2PF6 that feature terminal 2,2'-bipyridine groups were prepared and their self-assembly with Fe(NTf<sub>2</sub>)<sub>2</sub> or Fe(OTf) was performed which delivered tetrahedral assembly 12 and

cubic assembly **17** as evidenced by analysis of complexation induced changes in <sup>1</sup>H NMR chemical shift, DOSY, and ESI-MS results for **12**. Assemblies **12** and **17** are stable under aqueous conditions. Finally, threading of ligands **11** and **16** with CB[7] gave the acetonitrile soluble complexes CB[7]•**11**•2PF<sub>6</sub> and CB[7]•**16**•2PF<sub>6</sub> which underwent assembly with Fe(OTf)<sub>2</sub> in acetonitrile to give self assembled tetrahedron **13** and cube **18** which on average contain 1.80 and 6.59 CB[7] molecules, respectively. In conclusion, we find that the self-assembly of MOPs with mechanically interlocked CB[7] requires that the CB[7] units reside on the viologen unit which is favored in acetonitrile rather than the phenylene binding epitope. Our inability to achieve full binding of CB[7] to every MOP edge cannot be ascribed to steric effects but probably reflects partial dissociation of the CB[7]•**11** or CB[7]•**16** complexes under the reaction conditions. Future work targets new ligands with tighter binding and slower dissociating CB[n] binding domains that may assemble to give MOPs fully saturated with mechanically interlocked CB[n].

**Experimental Details.** Compounds **1**,(26) **2**,(27) and **10**(38) were prepared according to literature procedures. NMR spectra were measured on 400 MHz, 500 MHz, and 600 MHz spectrometers (400, 500, 600 MHz for <sup>1</sup>H NMR; 100, 126 MHz for <sup>13</sup>C NMR) at room temperature in the stated deuterated solvents unless otherwise stated. Low resolution mass spectrometry was performed using a JEOL AccuTOF electrospray instrument. Electrospray ionization-mass spectrometry (ESI-MS) for cage samples was performed on a Waters Synapt G2 mass spectrometer, using sample solutions (1 mg mL<sup>-1</sup>) in DMSO/CH<sub>3</sub>CN (1/1, v/v). The ESI-MS experiments were carried out under the following conditions: ESI capillary voltage, 3 kV; sample cone voltage, 30 V; extraction

cone voltage, 0.1 V; source temperature 100 °C; desolvation temperature, 100 °C; cone gas flow, 10 L/h; desolvation gas flow, 700 L/h ( $N_2$ ).

*Compound 3 (Chloride salt)*. Compound **1** (0.437 g, 0.778 mmol) was dissolved in EtOH (75.0 mL) and then **2** (0.446 g, 1.57 mmol) was added to the reaction flask causing the yellow solution to turn dark brown. The reaction mixture was stirred and heated at reflux overnight. The reaction mixture was allowed to cool to room temperature and then the majority of the solvent (20 mL remaining) was removed by rotary evaporation. The heterogenous mixture was then poured into THF (800 mL) and stirred at room temperature for 2 h which resulted in a brown precipitate. The solid was collected by filtration to afford **3** as a dark red powder (569 mg, 96% yield). M.p. > 300 °C. IR (ATR, cm<sup>-1</sup>) 3359m, 3030m, 1702m, 1630m, 1584m, 1529m, 1489m, 1367m, 1319m, 1234m, 1152s, 1053m, 818s. <sup>1</sup>H NMR (600 MHz, DMSO- $d_6$ ): 9.73 (d, J = 6.0 Hz, 4H), 9.57 (s, 2H), 9.09 (d, J = 6.0 Hz, 4H), 8.05 (d, J = 8.4 Hz, 4H), 8.03 (d, J = 8.4 Hz, 4H), 7.77 (d, J = 8.3Hz, 4H), 7.64 (d, J = 8.3Hz, 4H), 1.50 (s, 18H). <sup>13</sup>C NMR (126 MHz, DMSO- $d_6$ ): 152.8, 148.8, 145.7, 142.9, 140.7, 140.2, 131.4, 127.5, 127.4, 126.7, 125.3, 118.6, 79.4, 20.1. ESI-MS (ESI): m/z 346.3 ([M]<sup>2+</sup>), calcd. for C<sub>44</sub>H<sub>44</sub>N<sub>4</sub>O<sub>4</sub>, 346.4.

Compound 4 (Chloride salt). Compound 3 (0.301 g, 0.395 mmol) was suspended in CH<sub>2</sub>Cl<sub>2</sub> (30 mL) and the slurry was cooled in an ice-water bath. TFA (6.0 mL) was added dropwise over 30 minutes which resulted in a red solution. The solution was removed from the ice bath and stirred at room temperature for 2 hours. The solvent was removed by rotary evaporation yielding a dark yellow oil. The oil was treated with EtOH (10 mL) and then the solvent was removed by rotary evaporation which resulted in a purple gummy solid. Repetition of the treatment with EtOH two more times ultimately gave 4 as the dichloride salt as a dark yellow solid (0.367 g, 98%) after drying on high vacuum overnight. M.p. > 300 °C. IR (ATR, cm<sup>-1</sup>) 3400w, 2920w, 2851w, 1631m,

1608m, 1592m, 1492m, 1285w, 1199w, 824s. <sup>1</sup>H NMR (600 MHz, D<sub>2</sub>O): 9.43 (d, J = 6.9 Hz 4H), 8.78 (d, J = 6.9 Hz, 4H), 7.97 (d, J = 8.6 Hz, 4H), 7.87 (d, J = 8.6 Hz, 4H), 7.66 (d, J = 8.4 Hz, 4H), 6.98 (d, J = 8.4 Hz, 4H). <sup>13</sup>C NMR (100 MHz, D<sub>2</sub>O, Dioxane as reference): 150.6, 145.4, 143.1, 141.8, 129.2, 129.0, 127.2, 124.7, 123.5. ESI-MS (ESI, sample dissolved in H<sub>2</sub>O): m/z 246.1 ([M]<sup>2+</sup>), C<sub>34</sub>H<sub>28</sub>N<sub>4</sub>, calculated 246.3.

Compound 4 (Hexafluorophosphate salt). First, counter anion exchange from chloride to hexafluorophosphate was performed by dissolving 4 (9.1 mg, 11.5 μmol) in water (5.0 mL) and then adding NH<sub>4</sub>PF<sub>6</sub> (22.3 mg, 115 μmol) which caused a purple precipitate to form. The heterogenous mixture was sonicated for 30 minutes. The solid was obtained by centrifugation and the pellet was suspended in water (2.0 mL) with the help of vortexing and sonication and then the mixture was centrifuged. The supernatant was decanted. The process was repeated 3 times to ensure excess NH<sub>4</sub>PF<sub>6</sub> was removed followed by drying under high vacuum to give 4 (hexafluorophosphate salt, 7.1 mg, 9.1 μmol, 79%). M.p. > 300 °C. IR (ATR, cm<sup>-1</sup>) 3076m, 2833m, 2600m, 1740s, 1679s, 1634m, 1545w, 1520w, 1492m, 1433w, 1406w, 1224w, 1196s, 1131s, 1005w, 862w, 832w, 817m, 805m, 790m, 720m, 666m. <sup>1</sup>H NMR (600 MHz, CD<sub>3</sub>CN): 9.22 (d, J = 7.08 Hz, 4H), 8.65 (d, J = 7.08 Hz, 4H), 7.95 (d, J = 8.81 Hz, 4H), 7.80 (d, J = 8.81 Hz, 4H), 7.56 (d, J = 8.61 Hz, 4H), 6.79 (d, J = 8.61 Hz, 4H). <sup>13</sup>C NMR (126 MHz, DMSO- $d_6$ ): 149.7, 148.5, 145.4, 143.8, 139.6, 127.7, 126.5, 126.4, 125.0, 124.6, 114.2. ESI-MS (ESI, sample dissolved in CH<sub>3</sub>CN): m/z 246.2 ([M]<sup>2+</sup>), C<sub>34</sub>H<sub>28</sub>N<sub>4</sub>, calculated 246.3.

Compound 4 (Triflimide salt). First, counter anion exchange from chloride to triflimide was performed by dissolving 4 (11.6 mg, 12.3 μmol) in water (2.0 mL) and then adding LiNTf<sub>2</sub> (291 mg, 1.01 mmol) which caused a purple precipitate to form. Heterogenous mixture was sonicated for 30 minutes. The solid was obtained by centrifugation and the pellet was suspended in water

(2.0 mL) with the help of vortexing and sonication and then the mixture was centrifuged. The supernatant was decanted. The process was repeated 3 times to ensure excess LiNTf<sub>2</sub> was removed followed by drying under high vacuum to give **4** (triflimide salt, 10.7 mg, 10.2  $\mu$ mol, 83%). M.p. > 300 °C. IR (ATR, cm<sup>-1</sup>) 3648w, 3401w, 3126w, 2919m, 2851w, 2362w, 1632m, 1609m, 1593m, 1530w, 1492m, 1435w, 1410w, 1285w, 1199w, 1003w, 815s, 740w. <sup>1</sup>H NMR (400 MHz, CD<sub>3</sub>CN): 9.22 (d, J = 7.1 Hz, 4H), 8.65 (d, J = 7.1, Hz, 4H), 7.95 (d, J = 8.9, Hz, 4H), 7.80 (d, J = 8.9, Hz, 4H), 7.56 (d, J = 8.6 Hz, 4H), 6.79 (d, J = 8.6 Hz, 4H), 4.48 (br. s, 4H). <sup>13</sup>C NMR (126 MHz, CD<sub>3</sub>CN): 150.8, 150.2, 146.3, 146.0, 141.0, 129.2, 128.5, 128.3, 127.5, 125.8, 115.8. ESI-MS (ESI, sample dissolved in CH<sub>3</sub>CN): m/z 246.1 ([M]<sup>2+</sup>), C<sub>34</sub>H<sub>28</sub>N<sub>4</sub>, calculated 246.3.

Cage 6 (Hexafluorophosphate salt). Hexafluorophosphate salt 4 (10.4 mg, 13.3 μmol) and iron (II) triflate (3.1 mg, 8.8 μmol) were placed in a scintillation vial with a stir bar and capped with a rubber septum. The vial was purged of oxygen by several cycles of high vacuum and then refilling with N₂ gas. Subsequently, 5 (2.5 μL, 26 μmol) and dry acetonitrile (0.9 mL) were added by syringe. The reaction vial was sonicated for 30 minutes which resulted in a dark purple solution. The reaction mixture was then stirred at 60 °C for 24 h. After cooling to room temperature, Et₂O (6.0 mL) was added to the reaction mixture which caused 6 to precipitate. After centrifugation and decantation of the supernatant, 6 was obtained as a purple solid. Purple solid was redissolved in CH₃CN (0.5 mL) and excess NH₄PF₀ (4.4 mg, 27 μmol) was added. Et₂O (6.0 mL) was added to the solution causing 6 to precipitate. After centrifugation and decantation of the supernatant, 6•20PF₀ was air dried and obtained as a purple solid (9.3 mg, 90%). IR (ATR, cm⁻¹): 3125w, 3070w, 1633m, 1595w, 1488m, 1443w, 1400w, 1254m, 1223m, 1160m, 1028m, 1005w, 816s, 774m, 750w, 740w. ¹H NMR (400 MHz, CD₃CN): 9.24 (br. s, 24H), 8.95 − 8.90 (m, 12H), 8.68 (br. s, 24H), 8.58 (br. d, 12H), 8.44 (br. t, 12H), 8.09 (br. s, 24H), 7.93 (br. s, 24H), 7.82 (br. t,

12H), 7.70 – 7.65 (m, 24H), 7.50 – 7.45 (m, 12H), 5.60 - 5.55 (m, 24H). <sup>13</sup>C NMR (126 MHz, CD<sub>3</sub>CN): 175.9, 159.2, 157.1, 151.6, 151.5, 146.8, 144.0, 143.1, 140.9, 140.0, 132.6, 131.3, 130.3, 129.7, 128.7, 128.6, 126.3, 123.3.

*Cage 6 (Triflimide salt).* Triflimide salt **4** (5.7 mg, 5.4 μmol) was placed in a scintillation vial with a stir bar and iron (II) triflimide (2.6 mg, 4.2 μmol) and capped with a rubber septum. The vial was purged of oxygen by several cycles of high vacuum and then refilling with  $N_2$  gas. Subsequently, dry acetonitrile (1.0 mL) and **5** (0.5 μL, 5 μmol) was added by syringe. The reaction vial was sonicated for 30 minutes which resulted in a dark purple solution. The reaction mixture was then stirred at 60 °C for 24 h. After cooling to room temperature, Et<sub>2</sub>O (6.0 mL) was added to the reaction mixture which caused **6** to precipitate. After centrifugation and decantation of the supernatant, **6** was obtained as a purple solid which was air dried. <sup>1</sup>H NMR (600 MHz, CD<sub>3</sub>CN): 9.24 (br. s, 24H), 9.00 – 8.95 (m, 12H), 8.69 (br. m, 24H), 8.65 - 8.55 (br. m, 12H), 8.50 - 8.40 (br. m, 12H), 8.06 (d, J= 8.6 Hz, 24H), 7.93 (br. m, 24H), 7.83 (br. m, 12H), 7.75 – 7.60 (m, 24H), 7.55 – 7.45 (m, 12H), 5.70 - 5.60 (m, 24H). <sup>13</sup>C NMR (126 MHz, CD<sub>3</sub>CN): 175.9, 157.1, 151.7, 151.5, 151.4, 146.6, 144.0, 143.0, 140.9, 140.0, 132.5, 131.3, 130.1, 129.5, 128.49, 128.43, 126.2, 126.0, 125.4, 124.1, 123.3, 122.0, 119.9.

Cage 7 (Hexafluorophosphate salt). Solid CB[7] (3.0 mg, 2.6 μmol) and 4•2Cl (2.4 mg, 2.5 μmol) was dissolved in D<sub>2</sub>O (1.0 mL). The 1:1 stoichiometric ratio was confirmed by <sup>1</sup>H NMR integration of the resonances of CB[7] versus 4. An excess of NH<sub>4</sub>PF<sub>6</sub> (7.7 mg, 47 μmol) was added to the solution causing a dark brown solid to precipitate. The heterogenous mixture was sonicated for 30 minutes before being centrifuged and the supernatant was decanted. The moist solid was suspended in water with the help of sonication followed by centrifugation. The brown solid was dried on high vacuum overnight to give 4•CB[7] (4.6 mg, 90%). Solid 4•CB[7] (2.3 mg,

1.2 µmol) was placed in a scintillation vial with a stir bar and capped with a rubber septum. The vial was purged of oxygen by several cycles of high vacuum and then refilling with N<sub>2</sub> gas. Subsequently, 5 (0.2 μL, 2 μmol), a solution of iron (II) triflate (16 mM, 50 μL, 0.8 μmol) in dry acetonitrile, and dry acetonitrile (50 µL) was added by syringe. The reaction vial was sonicated for 30 minutes which gave a dark purple solution. The reaction was then stirred at 60 °C for 24 h. The reaction mixture was cooled to room temperature and then Et<sub>2</sub>O (6.0 mL) was added which resulted in a precipitate. The heterogenous mixture was centrifuged, the supernatant removed, and the pellet was dried in air to give 7 as a purple solid. Purple solid was redissolved in CH<sub>3</sub>CN (0.5 mL) and excess NH<sub>4</sub>PF<sub>6</sub> (2.0 mg, 12 μmol) was added. Et<sub>2</sub>O (6.0 mL) was added to the solution causing 7 to precipitate. After centrifugation and decantation of the supernatant, 7.20PF<sub>6</sub> was air dried and obtained as a purple solid (1.9 mg, 56%). IR (ATR, cm<sup>-1</sup>): 3366w, 3124w, 1738s, 11632m, 1595w, 1488m, 1464s, 1423m, 1375m, 1320m, 1278m, 1227s, 1189s, 1029m, 1005w, 968m, 830s, 800s, 756m, 672w. <sup>1</sup>H NMR (600 MHz, CD<sub>3</sub>CN, RT): 9.26 – 9.18 (m, 24H), 8.97 (br. m, 12H), 8.70 – 8.60 (m, 28H), 8.45 (br., 12H), 8.25 – 8.20 (m, 16H), 8.10 (br., 18H), 7.94 (br., 18H), 7.82 (br., 16H), 7.69 (br., 24H), 7.47 (br., 12H), 7.11 (br., 8H), 5.67 – 5.58 (m, 52H), 5.27 (s, 28H), 4.06 (d, J = 13.0 Hz, 28H). <sup>13</sup>C NMR (126 MHz, CD<sub>3</sub>CN): 190.3, 175.8, 159.2, 157.1, 156.3, 151.5, 148.9, 146.7, 144.0, 143.0, 142.8, 140.9, 140.0, 138.8, 132.5, 131.3, 130.3, 130.1, 129.6, 138.5, 128.1, 126.2, 126.0, 124.1, 123.2, 71.7, 53.4.

Cage 7 (Triflimide Salt). Solid CB[7] (6.2 mg, 5.3 μmol) and 4 (5.6 mg, 5.9 mmol) was dissolved in D<sub>2</sub>O (2.0 mL). The 1:1 stoichiometric ratio was confirmed by <sup>1</sup>H NMR integration of the resonances of CB[7] versus 4. An excess of LiNTf<sub>2</sub> (169 mg, 0.655 mmol) was added to the solution causing a dark brown solid to precipitate. The heterogenous mixture was sonicated for 30 minutes before being centrifuged and the supernatant was decanted. The moist solid was

suspended in water with the help of sonication followed by centrifugation. The brown solid was dried on high vacuum overnight to give  $4 \cdot \text{CB}[7]$  (12.3 mg, 94%). Solid  $4 \cdot \text{CB}[7]$  (6.1 mg, 2.8 µmol) was placed in a vial with a stir bar and iron (II) triflimide (1.3 mg, 2.1 µmol). The vial was capped with a rubber septum and deoxygenated by repeated cycles of high vacuum and then refilling with N<sub>2</sub> gas. Dry acetonitrile (0.6 mL) and 5 (0.3 µL, 3 µmol) were added by syringe. The reaction vial was sonicated for 30 minutes which gave a dark purple solution. The reaction was then stirred at 60 °C for 24 h. The reaction mixture was cooled to room temperature and then Et<sub>2</sub>O (6.0 mL) was added which resulted in a precipitate. The heterogenous mixture was centrifuged, the supernatant removed, and the pellet was dried in air to give 7 as a purple solid.  $^1\text{H}$  NMR (600 MHz, CD<sub>3</sub>CN, RT): 9.25 – 9.15 (m), 8.90 (br. m), 8.70 (br. s), 8.25 – 7.80 (m), 7.70 – 7.65 (m), 7.46 (br. s), 7.40 – 7.25 (m), 7.14 (br. s), 5.70 (d), 5.27 (br. s), 4.06 (d).  $^{13}\text{C}$  (126 MHz, CD<sub>3</sub>CN, RT): 156.3, 151.9, 148.9, 146.7, 131.4, 130.9, 130.4, 130.1, 128.3, 128.1, 128.0, 127.5, 127.3, 126.3, 126.1, 124.5, 124.2, 124.0, 122.0, 120.3, 119.9, 71.6, 53.4.

*Compound 11 (Chloride salt).* Compound 1 (0.205 g, 0.827 mmol) and 10 (0.211 mg, 0.376 mmol) were dissolved in EtOH (55.0 mL). The solution was heated at reflux for 24 h during which the solution turned brown in color. The reaction was then concentrated by rotary evaporation (to ≈ 20 mL) and then poured into THF (500 mL). After stirring for 2 hours at room temperature, a yellow precipitate was observed which was isolated by filtration. The crude solid was washed on the frit with THF (10 mL) three times to afford 11 as the chloride salt (259 mg, 97%). M.p. > 300 °C. IR (ATR, cm<sup>-1</sup>): 3368m, 3107w, 1628s, 1587m, 1460s, 1433s, 1417m, 1368m, 1342w, 1244m, 1093w, 1072w, 1034w, 1000s, 832s, 817s. <sup>1</sup>H NMR (600 MHz, DMSO- $d_6$ , RT): 9.80 (d, J = 6.4 Hz, 4H), 9.21 (s, 2H), 9.14 (d, J = 6.4 Hz, 4H), 8.76 (d, J = 6.5 Hz, 2H), 8.58 (d, J = 8.2 Hz, 2H), 8.48 (d, J = 6.5 Hz, 2H), 8.45 (d, J = 8.2 Hz, 2H), 8.30 (d, J = 8.3 Hz, 4H), 8.17 (d, J = 8.3 Hz, 2H), 8.48 (d, J = 6.5 Hz, 2H), 8.45 (d, J = 8.2 Hz, 2H), 8.30 (d, J = 8.3 Hz, 4H), 8.17 (d, J = 8.3 Hz, 4H), 8.18 (d, J = 8.3 Hz, 4H), 8.18

4H), 8.02 (t, J = 6.5 Hz, 2H), 7.52 (t, J = 6.5 Hz, 2H). <sup>13</sup>C NMR (126 MHz, DMSO- $d_6$ ): 155.1, 154.2, 149.4, 149.0, 147.7, 145.9, 139.9, 139.6 137.6, 135.7, 134.4, 128.5, 126.6, 125.7, 125.1 120.6. ESI-MS (ESI, sample dissolved in H<sub>2</sub>O): m/z 309.1 ([M]<sup>2+</sup>), C<sub>42</sub>H<sub>30</sub>N<sub>6</sub>, calculated 309.4.

Compound 11 (Hexafluorophosphate salt). Compound 11 (chloride) was transformed into the hexafluorophosphate salt by dissolving 11·2Cl (36.8 mg, 53.4 µmol) in water (12 mL) and heating to 80 °C followed by the addition of NH<sub>4</sub>PF<sub>6</sub> (90.7 mg, 556 mmol) was resulted in the formation of a precipitate. Heterogenous mixture was stirred at 80 °C for 30 minutes. The heterogenous mixture was cooled to room temperature, centrifuged, and the supernatant was decanted to give a moist solid. The moist solid was suspended in water (2.0 mL) with the help of sonication, followed by centrifugation, and removal of the supernatant. This process was repeated three times to remove excess NH<sub>4</sub>PF<sub>6</sub> and then the solid 11•2PF<sub>6</sub> was dried under high vacuum (39.1 mg, 81%). M.p. > 300 °C. IR (ATR, cm<sup>-1</sup>): 3135w, 3053w, 2924s, 2362w, 1636m, 1588m, 1552w, 1485w, 1458m, 1435m, 1417w, 1369w, 1264w, 1216w, 1149w, 1094w, 1067w, 1043w, 1002w, 877s, 794m, 752w, 741w, 716w, 695w. <sup>1</sup>H NMR (600 MHz, CD<sub>3</sub>CN, RT): 9.29 (d, J = 7.0, 4H), 9.10 (d, J =4.1 Hz, 2H), 8.75 - 8.70 (m, 6H), 8.61 (d, J = 9.5 Hz, 2H), 8.50 (d, J = 7.9, 2H), 8.29 (dd, J = 4.1, 9.5 Hz, 2H), 8.17 (d, J = 8.7 Hz, 4H), 8.00 - 1.90 (m, 6H), 7.45 (t, J = 4.8 Hz, 2H). <sup>13</sup>C NMR (126) MHz, CD<sub>3</sub>CN): 150.4, 148.9, 146.7, 143.0, 138.7, 137.3, 136.9, 130.2, 128.4, 126.3, 125.3, 121.9. ESI-MS (ESI, sample dissolved in CH<sub>3</sub>CN): m/z 309.0 ([M]<sup>2+</sup>), C<sub>42</sub>H<sub>30</sub>N<sub>6</sub>, calculated 309.4.

Compound 11 (Triflimide salt). Compound 11 (chloride) was transformed into the triflimide salt by dissolving 11·2Cl (23.9 mg, 34.7 μmol) in water (10 mL) and heating to 80 °C followed by the addition of LiNTf<sub>2</sub> (107.2 mg, 373 μmol) was resulted in the formation of a precipitate. Heterogenous mixture was stirred at 80 °C for 30 minutes. The heterogenous mixture was cooled to room temperature, centrifuged, and the supernatant was decanted to give a moist solid. The

moist solid was suspended in water (4.0 mL) with the help of sonication, followed by centrifugation, and removal of the supernatant. This process was repeated three times to remove excess LiNTf2 and then the solid **11** (29.2 mg, 71%) was dried under high vacuum. M.p. > 300 °C. IR (ATR, cm<sup>-1</sup>): 3124w, 3068w, 1632m, 1587w, 1573w, 1550w, 1485w, 1458m, 1436w, 1419w, 1351s, 1331s, 1179s, 1129s, 1093w, 1050s, 1000m, 877w, 828m, 799m, 756m, 739m.  $^{1}$ H NMR (400 MHz, CD<sub>3</sub>CN, RT): 9.29 (d, J = 6.7, 4H), 9.10 (d, J = 2.1 Hz, 2H), 8.75 - 8.70 (m, 6H), 8.61 (d, J = 8.3 Hz, 2H), 8.50 (d, J = 7.9, 2H), 8.29 (dd, J = 2.1, 8.3 Hz, 2H), 8.17 (d, J = 8.6 Hz, 4H), 8.00 - 1.90 (m, 6H), 7.45 (t, J = 5.1 Hz, 2H).  $^{13}$ C NMR (126 MHz, DMSO-d<sub>6</sub>): 155.1, 154.6, 149.5, 149.0, 147.7, 145.9, 141.9, 139.9, 137.5, 135.7, 133.7, 128.5, 126.6, 125.7, 124.5, 120.6, 118.4. ESI-MS (ESI, sample dissolved in CH<sub>3</sub>CN): m/z 309.0 ([M]<sup>2+</sup>), C<sub>42</sub>H<sub>30</sub>N<sub>6</sub>, calculated 309.4.

Cage 12 (Hexafluorophosphate salt). A solution of iron (II) triflate (10.7 mM, 0.5 mL, 5.37 μmol) in CH<sub>3</sub>CN was added to a vial with solid hexafluorophosphate salt 12 (5.7 mg, 6.27 μmol) suspended in CH<sub>3</sub>CN (1.0 mL). Once iron was added, the yellow suspension turned ruby red. The mixture was sonicated for 30 minutes and then stirred at 60 °C for 24 h resulting in a ruby red homogenous solution. The red solution was cooled to room temperature and then Et<sub>2</sub>O (6.5 mL) was added which resulted in a red solid. The heterogenous mixture was centrifuged followed by removal of the supernatant. The solid was resuspended in Et<sub>2</sub>O (6.0 mL) with the help of sonication followed by centrifugation and decantation of the supernatant to obtain the red solid. The process was repeated two more times. Red solid was then redissolved in a solution of NH<sub>4</sub>PF<sub>6</sub> (77 mM, 0.25 mL, 3.1 mmol) in CH<sub>3</sub>CN. Et<sub>2</sub>O (5.0 mL) was added causing 12 to precipitate. Red solid was collected by centrifugation and decantation. The solid was resuspended in Et<sub>2</sub>O (6.0 mL) with the help of sonication followed by centrifugation and decantation of the supernatant to obtain the red solid. The process was repeated two more times. Cage 12•20PF<sub>6</sub> was air dried and obtained

as a red solid (4.3 mg, 60%). IR (ATR, cm<sup>-1</sup>): 3657w, 3587w, 3129w, 2360w, 1634m, 1605w, 1490w, 1467m, 1440m, 1377w, 1344w, 1243w, 1168w, 1010w, 1008w, 815s, 752m, 738m. <sup>1</sup>H NMR (600 MHz, CD<sub>3</sub>CN, RT): 9.15 (d, J = 5.9 Hz, 24H), 8.74 (d, J = 8.3 Hz, 12H), 8.67 (d, J =8.3 Hz, 12H), 8.62 (d, J = 5.9 Hz, 24H), 8.52 (d, J = 8.7 Hz, 12H), 8.20 (t, J = 8.4 Hz, 12H), 7.84 (d, J = 5.68 Hz, 24H), 7.80-7.75 (m, 36H), 7.49 (m, 24H). <sup>13</sup>C NMR (126 MHz, CD<sub>3</sub>CN, RT): 160.0, 159.9, 155.5, 154.0, 151.6, 146.6, 143.8, 140.1, 139.7, 138.7, 138.4, 130.5, 128.9, 128.5, 126.4, 125.9, 125.1. ESI-MS: m/z 994.23 ([Fe<sub>4</sub>11<sub>6</sub> + 14PF<sub>6</sub>]<sup>6+</sup>),  $C_{252}H_{180}F_{84}Fe_4N_{36}P_{14}$ , calculated 994.13; 831.35 ( $[Fe_411_6 + 13PF_6]^{7+}$ ),  $C_{252}H_{180}F_{78}Fe_4N_{36}P_{13}$ , calculated 831.40; 709.30 ( $[Fe_411_6 + 13PF_6]^{7+}$ )  $12PF_6$ <sup>[8+</sup>),  $C_{252}H_{180}F_{72}Fe_4N_{36}P_{12}$ , calculated 709.35; 614.38  $([Fe_411_6]$  $11PF_6$ <sup>9+</sup>)  $C_{252}H_{180}F_{66}Fe_4N_{36}P_{11}$ , calculated 614.43.

Cage 12 (Triflimide salt). Triflimide salt 12 (16.0 mg, 13.6 μmol) was dissolved in CH<sub>3</sub>CN (3.4 mL) and then iron (II) triflimide (5.7 mg, 9.3 μmol) was added causing the solution to turn ruby red. The homogenous solution was sonicated for 30 minutes and then stirred at 70 °C for 24 h. The reaction mixture was cooled to room temperature and then Et<sub>2</sub>O (6.0 mL) was added which resulted in a red solid. The heterogenous mixture was centrifuged followed by removal of the supernatant. The solid was resuspended in Et<sub>2</sub>O (6.0 mL) with the help of sonication followed by centrifugation and decantation of the supernatant to obtain the red solid. The process was repeated two more times followed by air drying to obtain 12 as a red solid. <sup>1</sup>H NMR (400 MHz, CD<sub>3</sub>CN, RT): 9.11 (d, J = 6.7 Hz, 24H), 8.73 (d, J = 8.3 Hz, 12H), 8.66 (d, J = 8.3 Hz, 12H), 8.59 (d, J = 6.7 Hz, 24H), 8.50 (d, J = 8.4 Hz, 12H), 8.20 (t, J = 7.4 Hz, 12H), 7.85 - 7.70 (m, 60H), 7.49 (m, 24H). <sup>13</sup>C NMR (126 MHz, CD<sub>3</sub>CN, RT): 160.0, 159.7, 155.4, 151.5, 146.5, 143.7, 140.0, 139.6, 138.6, 138.2, 130.3, 128.9, 128.4, 126.3, 125.1, 121.9, 119.8.

Cage 12 (Sulfate salt). A solution of K<sub>2</sub>SO<sub>4</sub> (6.8 mg, 39 μmol) in D<sub>2</sub>O (500 μL) was treated with 12·2Cl (2.6 mg, 3.8 μmol) and FeSO<sub>4</sub>•7H<sub>2</sub>O (13mM, 200 μL, 2.5 μmol) dissolved in D<sub>2</sub>O. The reaction mixture was sonicated for 1 hour and then stirred at 50 °C for 24 hours during which the solution changed color from cloudy yellow to clear ruby red. Acetone (5.0 mL) was added to the reaction mixture which results in a red precipitate. The heterogeneous mixture was centrifuged, the supernatant decanted, and the pellet was air dried to give 12 as red solid. <sup>1</sup>H NMR (600 MHz, D<sub>2</sub>O, RT): 9.39 (d, J = 5.8 Hz, 24H), 8.88 (d, J = 7.6 Hz, 12H), 8.82 (br. s, 24H), 8.77 (d, J = 7.6 Hz, 12H), 8.61 (d, J = 7.9 Hz, 12H), 8.25 (br., 12H), 7.90 – 7.85 (m, 36H), 7.75 (d, J = 6.8 Hz, 12H), 7.70 (d, J = 7.44 Hz, 12H), 7.53 (br., 12H). <sup>13</sup>C NMR (126 MHz, D<sub>2</sub>O, Acetone as a standard, RT): 158.8, 158.2, 154.0, 151.2, 150.3, 145.0, 142.4, 138.7, 137.9, 137.5, 137.3, 128.7, 127.2, 126.9, 124.9, 124.1, 123.7.

Cage 13 (Hexafluorophosphate salt). A mixture of CB[7] (28.7 mg, 24.7 μmol) and 11·2CI (17.0 mg, 24.7 μmol) was dissolved in D<sub>2</sub>O (6.0 mL) using a heat gun and sonication and the 1:1 stoichiometric ratio was confirmed by measuring the <sup>1</sup>H NMR integrals for each component. The solution was heated to 80 °C and treated with NH<sub>4</sub>PF<sub>6</sub> (44.8 mg, 275 μmol) which caused the formation of an yellow precipitate. The heterogenous mixture was stirred at 80 °C for 30 minutes before cooling to room temperature, centrifuged, and the supernatant decanted. The moist solid was resuspended in water (2.0 mL) with the help of sonication followed by centrifugation and decantation. The process was repeated two more times and then the solid (44.1 mg, 86%) was dried on high vacuum overnight. A sample of 11•CB[7] hexafluorophosphate salt (2.3 mg, 1.1 μmol) was dissolved in CH<sub>3</sub>CN (0.15 mL) and then a solution of FeOTf<sub>2</sub> (50 μL, 16 mM in CH<sub>3</sub>CN) was added which caused the solution to turn ruby red. The reaction mixture was sonicated for 30 min, and then stirred at 60 °C for 24 h. The reaction mixture was cooled to room temperature

and then Et<sub>2</sub>O (7.0 mL) was added which resulted in a red precipitate. The red precipitate was obtained by centrifugation followed by decanting of the supernatant. The moist solid was resuspended in Et<sub>2</sub>O (2.0 mL) with the help of sonication followed by centrifugation and decantation of the supernatant. The process was repeated two more times and then air dried to give 13 as a red solid. Compound 13 was redissolved in CH<sub>3</sub>CN (0.5 mL) and excess NH<sub>4</sub>PF<sub>6</sub> (1.8 mg, 11 μmol) was added. Et<sub>2</sub>O (6.0 mL) was added to the solution causing 13 to precipitate. After centrifugation and decantation of the supernatant, 13.20PF<sub>6</sub> was collected as red solid. The red solid was resuspended in Et<sub>2</sub>O (2.0 mL) with the help of vortexing and collected by centrifugation and decantation. This process was repeated two additional time to ensure the removal of excess NH<sub>4</sub>PF<sub>6</sub>. The red solid was then air dried to yield 13•20PF<sub>6</sub>. IR (ATR, cm<sup>-1</sup>): 3493m, 3115w, 2920w, 2361w, 1733s, 1634m, 1465s, 1422m, 1375m, 1375m, 1320m, 1281m, 1227s, 1188s, 1029m, 967m, 823m, 801s, 757m, 671m. <sup>1</sup>H NMR (600 MHz, CD<sub>3</sub>CN, RT): 9.20 - 9.00 (m, 24H), 8.80 - 8.45 (m, 57H), 8.20 (br., 20H), 8.00 - 7.75 (m, 53H), 7.47 (br., 28H), 7.02 (br. s, 7H), 5.56(br., 26H), 5.35 – 5.15 (m, 26H), 4.01 (br., 26H). <sup>13</sup>C NMR (126 MHz, CD<sub>3</sub>CN, RT): 165.6, 160.2, 159.8, 156.2, 155.2, 151.4, 148.8, 146.6, 139.9, 139.2, 128.9, 128.4, 126.3, 123.9, 71.6, 53.4. ESI-MS: 1163.73 ([Fe<sub>4</sub>**11**<sub>6</sub> + 2CB[7] +  $13PF_6$ ]<sup>7+</sup>),  $C_{336}H_{264}F_{78}Fe_4N_{92}O_{28}P_{13}$ , calculated 1163.64; 1145.43 ([Fe<sub>4</sub>**11**<sub>6</sub> + 3CB[7] + 12PF<sub>6</sub>]<sup>8+</sup>),  $C_{378}H_{306}F_{72}Fe_4N_{120}O_{42}P_{12}$ , calculated 1145.48; 1002.16  $([Fe_411_6 + 3CB[7] + 11PF_6]^{9+})$ ,  $C_{378}H_{306}F_{66}Fe_4N_{120}O_{42}P_{11}$ , calculated 1002.10; 1000.27 ( $[Fe_411_6 + 6Fe_4N_{120}O_{42}P_{11}]$ )  $2CB[7] + 12PF_6]^{8+}$ ,  $C_{336}H_{264}F_{72}Fe_4N_{92}O_{28}P_{12}$ , calculated 1000.07; 887.3467 ([Fe<sub>4</sub>11<sub>6</sub> + 3CB[7] +  $10PF_6$ ]<sup>10+</sup>),  $C_{378}H_{306}F_{60}Fe_4N_{120}O_{42}P_{10}$ , calculated 887.39; 872.89 ([Fe<sub>4</sub>**11**<sub>6</sub> + 2CB[7] + 11PF<sub>6</sub>]<sup>9+</sup>),  $C_{336}H_{264}F_{66}F_{e4}N_{92}O_{28}P_{11}$ , calculated 872.84; 854.72 ([Fe<sub>4</sub>**11**<sub>6</sub> + 1CB[7] + 12PF<sub>6</sub>]<sup>8+</sup>),  $C_{294}H_{222}F_{72}Fe_4N_{64}O_{14}P_{12}$  calculated 854.77; 793.49 ([Fe<sub>4</sub>11<sub>6</sub> + 3CB[7] + 9PF<sub>6</sub>]<sup>11+</sup>),  $C_{378}H_{306}F_{54}Fe_4N_{120}O_{42}P_9$ , calculated 793.54; 771.11 ([Fe<sub>4</sub>**11**<sub>6</sub> + 2CB[7] + 10PF<sub>6</sub>]<sup>10+</sup>),

 $C_{336}H_{264}F_{60}Fe_4N_{92}O_{28}P_{10}, \quad calculated \quad 771.06; \quad 743.64 \quad ([Fe_4\mathbf{11}_6 \ + \ 1CB[7] \ + \ 11PF_6]^{9+}),$   $C_{294}H_{222}F_{66}Fe_4N_{64}O_{14}P_{11}, \quad calculated \quad 743.69.$ 

Cage 13 (Triflimide salt). A mixture of CB[7] (10.4 mg, 8.9 μmol) and 11·2Cl (6.2 mg, 9.0 μmol) was dissolved in D<sub>2</sub>O (7.0 mL) and the 1:1 stoichiometric ratio was confirmed by measuring the <sup>1</sup>H NMR integrals for each component. The solution was heated to 80 °C and treated with LiNTf<sub>2</sub> (0.5 mL, 0.2 mM in CH<sub>3</sub>CN) which caused the formation of an orange-brown precipitate. The heterogenous mixture was stirred at 80 °C for 30 minutes. The heterogenous mixture was cooled to room temperature, centrifuged, and the supernatant decanted. The moist solid was resuspended in water (1.0 mL) with the help of sonication followed by centrifugation and decantation. The process was repeated two more times and then the solid (16.5 mg, 81%) was dried on high vacuum overnight. A sample of 11 • CB[7] triflimide salt (7.9 mg, 4.3 µmol) was dissolved in CH<sub>3</sub>CN (0.5 mL) and then a solution of Fe(NTf<sub>2</sub>)<sub>2</sub> (0.5 mL, 6.2 mM in CH<sub>3</sub>CN) was added which caused the solution to turn ruby red. The reaction mixture was sonicated for 30 min. and then stirred at 70 °C for 24 h. The reaction mixture was cooled to room temperature and then Et<sub>2</sub>O (10.0 mL) was added which resulted in a red precipitate. The red precipitate was obtained by centrifugation followed by decanting of the supernatant. The moist solid was resuspended in Et<sub>2</sub>O (5.0 mL) with the help of sonication followed by centrifugation and decantation of the supernatant. The process was repeated two more times and then air dried to give 13 as a red solid. <sup>1</sup>H NMR (600 MHz, CD<sub>3</sub>CN, RT): 9.25-9.00 (br. m), 8.85-8.45 (m), 8.19 (br.s), 8.0-7.70 (br. m), 7.49 (br. m), 6.99 (br. s), 5.55 (br.), 5.17 (br.), 3.94 (br.). <sup>13</sup>C NMR (200 MHz, CD<sub>3</sub>CN, RT): 160.0, 156.2, 155.3, 153.7, 151.5, 149.0, 143.7, 140.0, 139.5, 138.6, 130.3, 128.9, 128.4, 126.3, 125.1, 123.7, 123.3, 121.7, 120.1, 71.5, 53.3.

Compound 15. A solution of H<sub>2</sub>O (16.7 mL), MeOH (5.1 mL), and THF (5.1 mL) was purged with N<sub>2</sub> for 15 min. and then compound 14 (0.154 g, 0.66 mmol), 9 (0.158 g, 0.72 mmol), and potassium carbonate (2.62 g, 29.2 mmol) were added to solution. The reaction mixture was heated and stirred at 70 °C under N<sub>2</sub> for 24 hours. The reaction mixture was then cooled to room temperature and solvents were removed under vacuum. The crude solid was dissolved in CH<sub>2</sub>Cl<sub>2</sub> (100 mL) and partitioned against aq. KOH (1 mM, 100 mL) in a separatory funnel. The organic layer was collected and dried over Na<sub>2</sub>SO<sub>4</sub> prior to removing the solvent by rotary evaporation. Compound 15 was purified by column chromatography (SiO<sub>2</sub>, DCM/EtOAc/NEt<sub>3</sub> 50:50:3). <sup>1</sup>H NMR analysis revealed residual triphenyl phosphine so the solid was triturated three times with hexanes (10 mL) to give 15 (0.103 g, 64%) as a brown solid. The <sup>1</sup>H NMR of 15 recorded in CDCl<sub>3</sub> matches with data reported previously.(43)

Compound 16 (Chloride salt). A suspension of 15 (95.0 mg, 0.38 mmol) and 1 (102 mg, 0.18 mmol) in EtOH (25 mL) was heated at reflux for 3 days during which the solution turned brown. The reaction mixture was concentrated by rotary evaporation (to ≈10 mL) and then poured into THF (200 mL) and then stirred for 2 hours which gave an orange-brown precipitate. The precipitate was obtained by filtration and then washed on the frit with THF (100 mL) to give 16 (96.0 mg, 77%) as an orange-brown solid. M.p. > 300 °C. IR (ATR, cm<sup>-1</sup>): 3368m, 3007w, 1629m, 1601m, 1601m, 1583m, 1546w, 1531w, 1512w, 1492w, 1459m, 1436m, 1386m, 1342w, 1257w, 991w, 825s, 810s.  $^{1}$ H NMR (400 MHz, DMSO- $d_6$ , RT) 9.80 (d, J = 5.6 Hz, 4H), 9.07 (d, J = 5.6 Hz, 4H), 8.89 (d, J = 6.1 Hz, 2H), 8.81 (s, 2H), 8.77 (d, J = 6.1 Hz, 2H), 8.49 (d, J = 6.1 Hz, 2H), 8.35 (d, J = 8.6 Hz, 2H), 8.19 (d, J = 8.6 Hz, 4H), 8.03 (dt, J = 6.1 and 1.8 Hz, 4H), 7.97 (dd, J = 6.1 and 1.8 Hz, 2H), 7.54 (dt, J = 6.1 and 1.8 Hz, 2H).  $^{13}$ C NMR (126 MHz, DMSO- $d_6$ ): 156.0, 154.7,

150.3, 149.2, 149.0, 146.5, 146.1, 142.8, 140.4, 137.7, 128.8, 126.4, 125.8, 124.7, 122.0, 120.9, 118.1. ESI-MS (ESI, sample dissolved in  $H_2O$ ): m/z 309.1 ([M]<sup>2+</sup>),  $C_{42}H_{30}N_6$ , calculated 309.4.

Compound 16 (Hexafluorophosphate salt). Compound 16 (chloride) was transformed into the hexafluorophosphate salt by dissolving 16.2Cl (15.4 mg, 22.3 µmol) in water (5.0 mL) and heating to 80 °C followed by the addition of NH<sub>4</sub>PF<sub>6</sub> (39.7 mg, 244 μmol) was resulted in the formation of a precipitate. Heterogenous mixture was stirred at 80 °C for 30 minutes. The heterogenous mixture was cooled to room temperature, centrifuged, and the supernatant was decanted to give a moist solid. The moist solid was suspended in water (2.0 mL) with the help of sonication, followed by centrifugation, and removal of the supernatant. This process was repeated three times to remove excess NH<sub>4</sub>PF<sub>6</sub> and then the solid **16**•2PF<sub>6</sub> (13.8 mg, 68%) was dried under high vacuum. M.p. > 300 °C. IR (ATR, cm<sup>-1</sup>): 3133w, 3070w, 2925w, 2361w, 2339w, 1733w, 1638m, 1602w, 1585m, 1568w, 1541w, 1515w, 1491w, 1460m, 1440m, 1387m, 1352w, 1216w, 1188w, 1132w, 1096w, 1039w, 1007w, 827s, 796s, 752w, 739w, 716w, 707w, 662w. <sup>1</sup>H NMR (600 MHz, CD<sub>3</sub>CN, RT): 9.29 (d, J = 6.5, 4H), 8.84 (m, 4H), 8.75 - 8.65 (m, 6H), 8.52 (d, J = 7.9 Hz, 2H), 8.23 (d, J = 8.4, 4H), 7.96 (m, 6H), 7.80 (d, J = 3.5 Hz, 2H), 7.46 (t, J = 5.0 Hz, 2H). <sup>13</sup>C NMR (126 MHz, CD<sub>3</sub>CN): 157.9, 156.4, 151.3, 150.4, 147.8, 146.8, 143.1, 138.4, 130.4, 128.4, 126.4, 125.5, 123.0, 122.0, 119.6. ESI-MS (ESI, sample dissolved in CH<sub>3</sub>CN): m/z 309.1 ([M]<sup>2+</sup>), C<sub>42</sub>H<sub>30</sub>N<sub>6</sub>, calculated 309.4.

Compound 16 (Triflimide salt). Counter anion exchange from chloride to triflimide was performed by dissolving 16·2Cl (16.3 mg, 23.6 μmol) in water (5 mL) and heated to 80 °C, followed by addition of excess LiNTf<sub>2</sub> (70.4 mg, 245 μmol) which resulted in the formation of an brown precipitate. The heterogenous mixture was centrifuged, the supernatant was decanted, and the moist solid was resuspended in water (4.0 mL) with the help of sonication followed by centrifugation and the decantation of the precipitate. The process was repeated 2 more times to

give **16**•2NTf<sub>2</sub> after drying under high vacuum (19.2 mg, 69%). M.p. > 300 °C. IR (ATR, cm<sup>-1</sup>): 3119w, 3064w, 1634m, 1601m, 1584m, 1547w, 1495w, 1472w, 1459w, 1432w, 1390w, 1347s, 1226m, 1174s, 1130s, 1051s, 1006w, 993w, 826m, 790m, 762w,790m, 762w, 739m, 706w. <sup>1</sup>H NMR (600 MHz, CD<sub>3</sub>CN, RT): 9.28 (d, J = 6.8, 4H), 8.84 (m, 4H), 8.75 - 8.65 (m, 6H), 8.52 (d, J = 8.0 Hz, 2H), 8.23 (d, J = 8.6, 4H), 7.97 (m, 6H), 7.80 (dd, J = 1.6, 5.0 Hz, 2H), 7.46 (t, J = 5.0 Hz, 2H). <sup>13</sup>C NMR (126 MHz, CD<sub>3</sub>CN): 151.4, 151.2, 150.2, 147.9, 146.7, 143.7, 143.0, 138.7, 130.4, 128.5, 126.4, 125.5, 123.1, 122.1, 122.0, 119.9, 119.7. ESI-MS (ESI, sample dissolved in CH<sub>3</sub>CN): m/z 309.1 ([M]<sup>2+</sup>), C<sub>42</sub>H<sub>30</sub>N<sub>6</sub>, calculated 309.4.

Cubic Cage 17 (Hexafluorophosphate salt). The obtained hexafluorophosphate salt of 17 (5.7 mg, 26.3 µmol) was dissolved in CH<sub>3</sub>CN (1.0 mL) followed by the addition of iron (II) triflate (10.7 mM, 0.5 mL, 5.4 µmol) in CH<sub>3</sub>CN which resulted in a color change to dark purple. The reaction mixture was sonicated for 30 minutes followed by stirring at 60 °C for 24 h. The reaction mixture is cooled to room temperature and then Et<sub>2</sub>O (6.0 mL) is added which results in a purple precipitate. The heterogenous mixture is centrifuged, the supernatant decanted, and the moist solid is resuspended in Et<sub>2</sub>O (6.0 mL) with the help of sonication followed by centrifugation and decantation. The process is repeated two more times. Compound 17 was redissolved in CH<sub>3</sub>CN (0.5 mL) and excess NH<sub>4</sub>PF<sub>6</sub> (12.9 mg, 79.1 µmol) was added. Et<sub>2</sub>O (6.0 mL) was added to the solution causing 17 to precipitate. After centrifugation and decantation of the supernatant, 17.40PF<sub>6</sub> was collected as purple solid. The purple solid was resuspended in Et<sub>2</sub>O (2.0 mL) with the help of vortexing and collected by centrifugation and decantation. This process was repeated two additional time to ensure the removal of excess NH<sub>4</sub>PF<sub>6</sub>. The purple solid was then air dried to yield 17.40PF<sub>6</sub> (7.2 mg, 78%). IR (ATR, cm<sup>-1</sup>): 3124w, 2087w, 1633w, 1615w, 1476w, 1440w, 1400w, 1218w, 1029w, 817s, 739m. <sup>1</sup>H NMR (600 MHz, CD<sub>3</sub>CN, RT): 9.30 (br. s, 48H), 8.96

(br. s, 24H), 8.84 (br. s, 24H), 8.74 (br. s, 48H), 8.30 – 8.24 (m, 72H), 8.06 (br. s, 48H), 7.81 (br. s, 24H), 7.62 – 7.53 (m, 72H). <sup>13</sup>C NMR (126 MHz, CD<sub>3</sub>CN, RT): 165.7, 161.1, 157.5, 155.6, 151.8, 149.4, 146.8, 144.6, 140.2, 130.8, 128.6, 126.7.

Cubic Cage 17 (Triflimide salt). The obtained triflimide salt of 17 (15.3 mg, 13.0 μmol) was dissolved in CH<sub>3</sub>CN (3.3 mL) followed by the addition of iron (II) triflimide (5.3 mg, 8.6 μmol) which resulted in a color change to dark purple. The reaction mixture was sonicated for 30 minutes followed by stirring at 70 °C for 24 h. The reaction mixture is cooled to room temperature and then Et<sub>2</sub>O (7.0 mL) is added which results in a red precipitate. The heterogenous mixture is centrifuged, the supernatant decanted, and the moist solid is resuspended in Et<sub>2</sub>O (6.0 mL) with the help of sonication followed by centrifugation and decantation. The process is repeated two more times and then solid 17 is air dried. <sup>1</sup>H NMR (400 MHz, CD<sub>3</sub>CN, RT): 9.29 (br. s, 48H), 8.94 (br. m, 24H), 8.83 (br. m, 24H), 8.72 (br., 48H), 8.35 – 8.20 (m, 72H), 8.04 (br., 48H), 7.79 (br. s, 24H), 7.70 – 7.45 (m, 72H). <sup>13</sup>C NMR (126 MHz, CD<sub>3</sub>CN, RT): 160.9, 159.9, 158.9, 155.4, 151.5, 149.7, 146.7, 144.4, 140.3, 139.9, 130.7, 128.4, 126.6, 123.3, 121.8, 119.7, 177.6.

Cubic Cage with CB[7] (18·40PF<sub>6</sub>). A mixture of CB[7] (22.7 mg, 19.5 μmol) and 16·2Cl (13.4 mg, 19.4 μmol) was dissolved in D<sub>2</sub>O (5.0 mL) by sonication and using a heat gun. The 1:1 stoichiometric ratio was confirmed by the integrals for each component in the <sup>1</sup>H NMR spectrum. The solution was heated to 80 °C and treated with NH<sub>4</sub>PF<sub>6</sub> (32.4 mg, 199 μmol) which caused the formation of a tan precipitate. The heterogenous mixture continued to stir at 80 °C for 30 minutes. The heterogenous mixture was centrifuged, the supernatant decanted, and the moist solid was resuspended in water (2.0 mL) followed by centrifugation and decantation two additional times. The solid was then dried at high vacuum overnight to yield the triflimide salt (34.0 mg, 85%). Complex 16·CB[7] hexafluorophosphate salt (3.3 mg, 0.16 μmol) was dissolved in CH<sub>3</sub>CN (1.0

mL). The solution was treated with Fe(OTf)<sub>2</sub> (22 mM, 50 μL, 0.11 μmol) dissolved in acetonitrile which gave a dark purple solution when added. The reaction mixture was sonicated for 30 min. and then stirred at 70 °C for 24 h. The reaction mixture is cooled to room temperature and then Et<sub>2</sub>O (6.0 mL) is added which results in a purple precipitate. The heterogenous mixture is centrifuged, the supernatant decanted, and the moist solid is then resuspended in Et<sub>2</sub>O followed by centrifugation and decantation of the precipitate. Compound 18 was redissolved in CH<sub>3</sub>CN (0.5 mL) and excess NH<sub>4</sub>PF<sub>6</sub> (1.0 mg, 6.1 µmol) was added. Et<sub>2</sub>O (6.0 mL) was added to the solution causing 18 to precipitate. After centrifugation and decantation of the supernatant, 18.40PF<sub>6</sub> was collected as purple solid. The purple solid was resuspended in Et<sub>2</sub>O (2.0 mL) with the help of vortexing and collected by centrifugation and decantation. This process was repeated two additional time to ensure the removal of excess NH<sub>4</sub>PF<sub>6</sub>. The purple solid was then air dried to yield **18**•40PF<sub>6</sub>. IR (ATR, cm<sup>-1</sup>): 3486m, 3123w, 2916m, 2849w, 2362w, 2338w,1735s, 1631m, 1463s, 1423m, 1375m, 1319m,1280m, 1227s, 1188s, 1029m, 967m, 841m, 822m, 800s, 757m, 671w. <sup>1</sup>H NMR (600 MHz, CD<sub>3</sub>CN, RT): 9.30 (d, J = 5.6 Hz), 9.00 - 8.65 (m), 8.50 - 8.00 (m), 8.00 - 7.40 (m), 5.75 - 5.55 (br. m), 5.35 - 5.15 (br. m), 4.10 - 3.90 (br. m). <sup>13</sup>C NMR (126 MHz, CD<sub>3</sub>CN, RT): 161.3, 159.8, 156.2, 148.8, 146.6, 144.5, 140.6, 139.7, 130.6, 128.4, 126.5, 124.0, 121.8, 119.7, 71.5, 53.2.

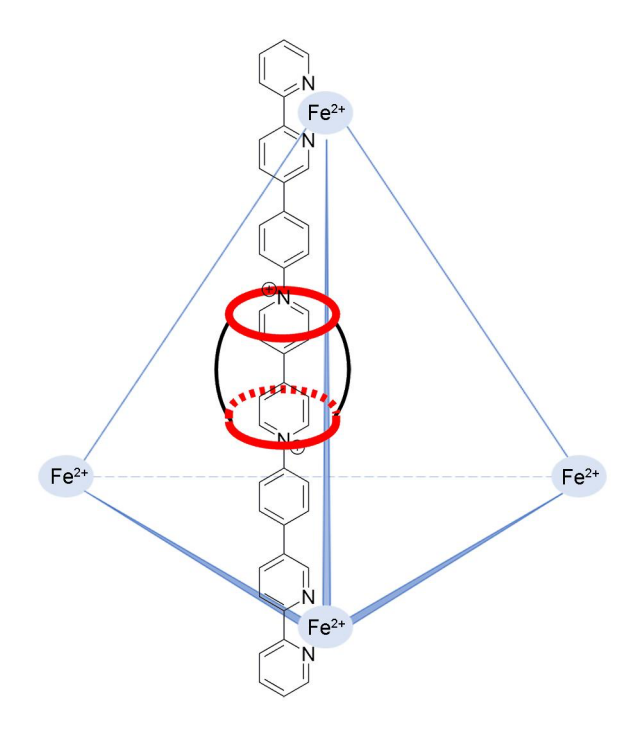
Cubic Cage with CB[7] (18·40NTf<sub>2</sub>). A mixture of CB[7] (13.8 mg, 11.9 μmol) and 16·2Cl (9.6 mg, 13.9 μmol) was dissolved in D<sub>2</sub>O (4.0 mL) and the 1:1 stoichiometric ratio was confirmed by the integrals for each component in the <sup>1</sup>H NMR spectrum. Solid LiNTf<sub>2</sub> (43.6 mg, 152 μmol) was added to the solution which resulted in the formation of a precipitate. The heterogenous mixture was centrifuged, the supernatant decanted, and the moist solid was resuspended in water (2.0 mL) followed by centrifugation and decantation. The solid was then dried at high vacuum overnight to

yield the triflimide salt (25.0 mg, 97%). Complex **16·CB[7]** triflimide salt (7.3 mg, 3.9 μmol) and Fe(NTf<sub>2</sub>)<sub>2</sub> (1.8 mg, 2.9 μmol) were dissolved in CH<sub>3</sub>CN (1.0 mL) which gave a dark purple solution. The reaction mixture was sonicated for 30 min. and then stirred at 70 °C for 24 h. The reaction mixture is cooled to room temperature and then Et<sub>2</sub>O (6.0 mL) is added which results in a purple precipitate. The heterogenous mixture is centrifuged, the supernatant decanted, and the moist solid is then resuspended in Et<sub>2</sub>O followed by centrifugation and decantation of the precipitate. The process is repeated two more times followed by air drying to give **18·**40(NTf<sub>2</sub>)<sup>-</sup> as a purple solid. <sup>1</sup>H NMR (400 MHz, CD<sub>3</sub>CN, RT): 9.29 (br. s), 9.00 - 8.60 (m), 8.45 – 7.95 (m), 7.95 – 7.40 (m), 5.75 - 5.55 (br. m), 5.35 - 5.15 (br. m), 4.10 - 3.90 (br. m). <sup>13</sup>C NMR (126 MHz, CD<sub>3</sub>CN, RT): 161.3, 159.8, 156.2, 148.8, 146.6, 144.5, 140.6, 139.7, 130.6, 128.4, 126.5, 124.0, 121.8, 119.7, 71.5, 53.2.

**Disclosure Statement.** The authors have no competing interests to declare.

**Funding.** We thank the National Institutes of Health (CA226830) and the National Science Foundation (CHE1807486) for financial support. K.B. thanks the University of Maryland for a Department of Education GAANN fellowship (P200A150033).

## **Table of Contents Graphic**



## References.

1) a) Barrow, S. J.; Kasera, S.; Rowland, M. J.; del Barrio, J.; Scherman, O. A., *Chem. Rev.* **2015**, *115*, 12320-12406; b) Rekharsky, M. V.; Inoue, Y., *Chem. Rev.* **1998**, *98*, 1875-1917; c) Diederich, F., *Angew. Chem., Intl. Ed. Engl.* **1988**, *27*, 362-386; d) Dale, E. J.; Vermeulen, N. A.; Juricek, M.; Barnes, J. C.; Young, R. M.; Wasielewski, M. R.; Stoddart, J. F., *Acc. Chem. Res.* **2016**, *49*, 262-273; e) Gutsche, C. D., *Acc. Chem. Res.* **1983**, *16*, 161-170; f) Cram, D. J., *Angew. Chem. Int. Ed.* **1988**, *27*, 1009-1020; g) Ogoshi, T.; Yamagishi, T.-A.; Nakamoto, Y., *Chem. Rev.* **2016**, *116*, 7937-8002; h) Xue, M.; Yang, Y.; Chi, X.; Zhang, Z.; Huang, F., *Acc. Chem. Res.* **2012**, *45*, 1294-1308; i) Wu, J.-R.; Yang, Y.-W., *Chem. Commun.* **2019**, *55*, 1533-1543. 2) a) Stella, V. J.; Rao, V. M.; Zannou, E. A.; Zia, V., *Adv. Drug Delivery Rev.* **1999**, *36*, 3-16; b) Ghale, G.; Nau, W. M., *Acc. Chem. Res.* **2014**, *47*, 2150-2159; c) Yu, Y.; Rebek, J., *Acc. Chem. Res.* **2018**, *51*, 3031-3040; d) Anslyn, E. V., *J. Org. Chem.* **2007**, *72*, 687-699; e) Meadows, M. K.; Anslyn, E. V., *Macrocyclic Supramol. Chem.* **2016**, 92-126; f) Walker, S.; Oun, R.; McInnes, F. J.; Wheate, N. J., *Isr. J. Chem.* **2011**, *51*, 616-624; g) Ma, X.; Zhao, Y., *Chem. Rev.* **2015**, *115*, 7794-7839; h) Zhang, H.; Liu, Z.; Zhao, Y., *Chem. Soc. Rev.* **2018**, *47*, 5491-5528.

3) a) Ogoshi, T.; Harada, A., Sensors **2008**, 8, 4961-4982; b) Border, S. E.; Pavlovic, R. Z.; Zhiquan, L.; Badjic, J. D., J. Am. Chem. Soc. **2017**, 139, 18496-18499; c) Wang, W.; Finnegan, T. J.; Lei, Z.; Zhu, X.; Moore, C. E.; Shi, K.; Badjic, J. D., Chem. Commun. **2020**, 56, 1271-1274; d) Zhou, J.; Yu, G.; Huang, F., Chem. Soc. Rev. **2017**, 46, 7021-7053; e) Zhang, X.; Cheng, Q.; Li, L.; Shangguan, L.; Li, C.; Li, S.; Huang, F.; Zhang, J.; Wang, R., Theranostics **2019**, 9, 3107-3121; f) Huang, Q.; Zhao, H.; Shui, M.; Guo, D.-S.; Wang, R., Chem. Sci. **2020**,

- 11, 9623-9629; g) Chang, Y.; Chen, J.-Y.; Yang, J.; Lin, T.; Zeng, L.; Xu, J.-F.; Hou, J.-L.; Zhang, X., ACS Appl. Mater. Interfaces **2019**, 11, 38497-38502; h) Kassem, S.; van Leeuwen, T.; Lubbe, A. S.; Wilson, M. R.; Feringa, B. L.; Leigh, D. A., Chem. Soc. Rev. **2017**, 46, 2592-2621.
- 4) a) Adam, J. M.; Bennett, D. J.; Bom, A.; Clark, J. K.; Feilden, H.; Hutchinson, E. J.; Palin, R.; Prosser, A.; Rees, D. C.; Rosair, G. M.; Stevenson, D.; Tarver, G. J.; Zhang, M.-Q., *J. Med. Chem.* **2002**, *45*, 1806-1816; b) Bom, A.; Bradley, M.; Cameron, K.; Clark, J. K.; Van Egmond, J.; Feilden, H.; MacLean, E. J.; Muir, A. W.; Palin, R.; Rees, D. C.; Zhang, M.-Q., *Angew. Chem., Int. Ed.* **2002**, *41*, 265-270; c) Trinh, T.; Cappel, J. P.; Geis, P. A.; McCarty, M. L.; Pilosof, D.; Zwerdling, S. S. (Procter and Gamble Company, USA .), Uncomplexed cyclodextrin solutions for odor control on inanimate surfaces, especially fabrics. WO9605358A1, 1996; d) Stella, V. J.; Rajewski, R. A., *Pharm. Res.* **1997**, *14*, 556-567.
- 5) a) Lagona, J.; Mukhopadhyay, P.; Chakrabarti, S.; Isaacs, L., *Angew. Chem. Int. Ed.* **2005**, *44*, 4844-4870; b) Nau, W. M.; Florea, M.; Assaf, K. I., *Isr. J. Chem.* **2011**, *51*, 559-577; c) Masson, E.; Ling, X.; Joseph, R.; Kyeremeh-Mensah, L.; Lu, X., *RSC Adv.* **2012**, *2*, 1213-1247; d) Shetty, D.; Khedkar, J. K.; Park, K. M.; Kim, K., *Chem. Soc. Rev.* **2015**, *44*, 8747-8761; e) Barrow, S. J.; Kasera, S.; Rowland, M. J.; del Barrio, J.; Scherman, O. A., *Chem. Rev.* **2015**, *115*, 12320-12406.
- 6) Lee, J. W.; Samal, S.; Selvapalam, N.; Kim, H.-J.; Kim, K., Acc. Chem. Res. 2003, 36, 621-630.
- 7) a) Bush, M. E.; Bouley, N. D.; Urbach, A. R., *J. Am. Chem. Soc.* **2005**, *127*, 14511-14517; b) Smith, L. C.; Leach, D. G.; Blaylock, B. E.; Ali, O. A.; Urbach, A. R., *J. Am. Chem. Soc.* **2015**, *137*, 3663-3669; c) Bosmans, R. P. G.; Briels, J. M.; Milroy, L.-G.; de Greef, T. F. A.; Merkx, M.; Brunsveld, L., *Angew. Chem., Int. Ed.* **2016**, *55*, 8899-8903; d) Dsouza, R. N.; Pischel, U.; Nau, W. M., *Chem. Rev.* **2011**, *111*, 7941-7980; e) Liu, S.; Ruspic, C.; Mukhopadhyay, P.; Chakrabarti, S.; Zavalij, P. Y.; Isaacs, L., *J. Am. Chem. Soc.* **2005**, *127*, 15959-15967; f) Macartney, D. H., *Isr. J. Chem.* **2011**, *51*, 600-615; g) Gamal-Eldin, M. A.; Macartney, D. H., *Can. J. Chem.* **2014**, *92*, 243-249; h) Ganapati, S.; Grabitz, S. D.; Murkli, S.; Scheffenbichler, F.; Rudolph, M. I.; Zavalij, P. Y.; Eikermann, M.; Isaacs, L., *ChemBioChem* **2017**, *18*, 1583-1588; i) Kaifer, A. E., *Acc. Chem. Res.* **2014**, *47*, 2160-2167; j) Ko, Y. H.; Kim, E.; Hwang, I.; Kim, K., *Chem. Commun.* **2007**, 1305-1315.
- 8) Zhang, X.; Xu, X.; Li, S.; Wang, L.-H.; Zhang, J.; Wang, R., Sci. Rep. 2018, 8, 1-7.
- 9) Cao, L.; Sekutor, M.; Zavalij, P. Y.; Mlinaric-Majerski, K.; Glaser, R.; Isaacs, L., *Angew. Chem. Int. Ed.* **2014**, *53*, 988-993.
- 10) a) Isaacs, L., *Acc. Chem. Res.* **2014**, *47*, 2052-2062; b) Del Barrio, J.; Horton, P.; Lairez, D.; Lloyd, G.; Toprakcioglu, C.; Scherman, O., *J. Am. Chem. Soc.* **2013**, *135*, 11760-11763.
- 11) a) Gao, C.; Kwong, C. H. T.; Sun, C.; Li, Z.; Lu, S.; Yang, Y.-W.; Lee, S. M. Y.; Wang, R., *ACS Appl. Mater. Interfaces* **2020**, *12*, 25604-25615; b) Ma, D.; Zhang, B.; Hoffmann, U.; Sundrup, M. G.; Eikermann, M.; Isaacs, L., *Angew. Chem. Int. Ed.* **2012**, *51*, 11358-11362; c) Yang, H.; Yuan, B.; Zhang, X.; Scherman, O. A., *Acc. Chem. Res.* **2014**, *47*, 2106-2115; d) Liu, J.; Lan, Y.; Yu, Z.; Tan, C. S. Y.; Parker, R. M.; Abell, C.; Scherman, O. A., *Acc. Chem. Res.* **2017**, *50*, 208-217.
- 12) Aqdot home page. <a href="https://aqdot.com">https://aqdot.com</a> (accessed May 6, 2020).
- 13) Rebek, J., Acc. Chem. Res. 2009, 42, 1660-1668.
- 14) Jordan, J. H.; Gibb, B. C., Chem. Soc. Rev. 2015, 44, 547-585.

- 15) a) Yoshizawa, M.; Klosterman, J. K.; Fujita, M., *Angew. Chem. Int. Ed.* **2009**, *48*, 3418-3438; b) Chakrabarty, R.; Mukherjee, P. S.; Stang, P. J., *Chem. Rev.* **2011**, *111*, 6810-6918; c) Brown, C. J.; Toste, F. D.; Bergman, R. G.; Raymond, K. N., *Chem. Rev.* **2015**, *115*, 3012-3035; d) Furukawa, H.; Cordova, K. E.; O'Keeffe, M.; Yaghi, O. M., *Science* **2013**, *341*, 1230444; e) Zarra, S.; Wood, D. M.; Roberts, D. A.; Nitschke, J. R., *Chem. Soc. Rev.* **2015**, *44*, 419-432. 16) a) Della Rocca, J.; Liu, D.; Lin, W., *Acc. Chem. Res.* **2011**, *44*, 957-968; b) Sumida, K.; Rogow, D. L.; Mason, J. A.; McDonald, T. M.; Bloch, E. D.; Herm, Z. R.; Bae, T.-H.; Long, J. R., *Chem. Rev.* **2012**, *112*, 724-781.
- 17) a) Wilson, B. H.; Loeb, S. J., *Chem* **2020**, *6*, 1604-1612; b) Roy, I.; Limketkai, B.; Botros, Y. Y.; Stoddart, J. F., *Acc. Chem. Res.* **2020**, *53*, 2762; c) Li, Q.; Zhang, W.; Miljanic, O. S.; Sue, C.-H.; Zhao, Y.-L.; Liu, L.; Knobler, C. B.; Stoddart, J. F.; Yaghi, O. M., *Science (Washington, DC, U. S.)* **2009**, *325*, 855-859; d) Li, Q.; Sue, C.-H.; Basu, S.; Shveyd, A. K.; Zhang, W.; Barin, G.; Fang, L.; Sarjeant, A. A.; Stoddart, J. F.; Yaghi, O. M., *Angew. Chem., Int. Ed.* **2010**, *49*, 6751-6755, S6751/6751-S6751/6719.
- 18) a) Tian, J.; Zhou, T.-Y.; Zhang, S.-C.; Aloni, S.; Altoe, M. V.; Xie, S.-H.; Wang, H.; Zhang, D.-W.; Zhao, X.; Liu, Y.; Li, Z.-T., *Nat. Commun.* **2014**, *5*, 5574; b) Tian, J.; Xu, Z.-Y.; Zhang, D.-W.; Wang, H.; Xie, S.-H.; Xu, D.-W.; Ren, Y.-H.; Wang, H.; Liu, Y.; Li, Z.-T., *Nat. Commun.* **2016**, *7*, 11580; c) Zhang, Y.-C.; Xu, Z.-Y.; Wang, Z.-K.; Wang, H.; Zhang, D.-W.; Liu, Y.; Li, Z.-T., *ChemPlusChem* **2020**, *85*, 1498-1503.
- 19) Das, G.; Sharma, S. K.; Prakasam, T.; Gandara, F.; Mathew, R.; Alkhatib, N.; Saleh, N. i.; Pasricha, R.; Olsen, J.-C.; Baias, M.; Kirmizialtin, S.; Jagannathan, R.; Trabolsi, A., *Commun. Chem.* **2019**, *2*, 1-9.
- 20) a) Mal, P.; Breiner, B.; Rissanen, K.; Nitschke, J. R., *Science* **2009**, *324*, 1697; b) Benyettou, F.; Prakasam, T.; Ramdas Nair, A.; Witzel, I.-I.; Alhashimi, M.; Skorjanc, T.; Olsen, J.-C.; Sadler, K. C.; Trabolsi, A., *Chem. Sci.* **2019**, *10*, 5884-5892; c) Zheng, Y.-R.; Suntharalingam, K.; Johnstone, T. C.; Lippard, S. J., *Chem. Sci.* **2015**, *6*, 1189-1193; d) Qiao, Y.; Zhang, L.; Li, J.; Lin, W.; Wang, Z., *Angew. Chem., Int. Ed.* **2016**, *55*, 12778-12782.
- 21) Samanta, S. K.; Moncelet, D.; Briken, V.; Isaacs, L., J. Am. Chem. Soc. 2016, 138, 14488-14496.
- 22) a) Samanta, S. K.; Quigley, J.; Vinciguerra, B.; Briken, V.; Isaacs, L., *J. Am. Chem. Soc.* **2017**, *139*, 9066-9074; b) Samanta, S. K.; Moncelet, D.; Vinciguerra, B.; Briken, V.; Isaacs, L., *Helv. Chim. Acta* **2018**, *101*, e1800057.
- 23) a) Nitschke, J. R., *Acc. Chem. Res.* **2007**, *40*, 103-112; b) Castilla, A. M.; Ramsay, W. J.; Nitschke, J. R., *Acc. Chem. Res.* **2014**, *47*, 2063-2073.
- 24) a) Rodríguez, J.; Mosquera, J.; Couceiro, J. R.; Nitschke, J. R.; Vázquez, M. E.; Mascareñas, J. L., J. Am. Chem. Soc. 2017, 139, 55-58; b) Riddell, I. A.; Smulders, M. M. J.; Clegg, J. K.; Nitschke, J. R., Chem. Commun. 2011, 47, 457-459; c) Bolliger, J. L.; Belenguer, A. M.; Nitschke, J. R., Angew. Chem. Int. Ed. 2013, 52, 7958-7962; d) Neelakandan, P. P.; Jiménez, A.; Nitschke, J. R., Chem. Sci. 2014, 5, 908-915; e) Foster, J. A.; Parker, R. M.; Belenguer, A. M.; Kishi, N.; Sutton, S.; Abell, C.; Nitschke, J. R., J. Am. Chem. Soc. 2015, 137, 9722-9729. 25) a) Biedermann, F.; Scherman, O. A., J. Phys. Chem. B 2012, 116, 2842-2849; b) Ong, W.; Gómez-Kaifer, M.; Kaifer, A. E., Org. Lett. 2002, 4, 1791-1794; c) Ong, W.; Kaifer, A. E., J. Org. Chem. 2004, 69, 1383-1385; d) Wang, W.; Kaifer, A. E., Supramol. Chem. 2010, 22, 710-
- 26) Kamogawa, H.; Sato, S., Bull. Chem. Soc. Japan 1991, 64, 321-323.

716.

27) Fischer-Durand, N.; Rejeb, S. B.; Le Goffic, F., Synth. Commun. 1998, 28, 963-970.

- 28) Cheng, W.-C.; Kurth, M. J., Org. Prep. Proced. Int. 2002, 34, 585,587-608.
- 29) Percástegui, E. G.; Mosquera, J.; Nitschke, J. R., Angew. Chem. Int. Ed. 2017, 56, 9136-9140.
- 30) Schultz, D.; Nitschke, J. R., Angew. Chem. Int. Ed. 2006, 45, 2453-2456.
- 31) a) Meng, W.; Clegg, J. K.; Thoburn, J. D.; Nitschke, J. R., J. Am. Chem. Soc. 2011, 133,
- 13652-13660; b) Ronson, T. K.; Meng, W.; Nitschke, J. R., J. Am. Chem. Soc. 2017, 139, 9698-9707.
- 32) Avram, L.; Cohen, Y., Chem. Soc. Rev. 2015, 44, 586-602.
- 33) Einstein, A., Annalen der Physik 1905, 322, 549-560.
- 34) Mock, W. L.; Shih, N. Y., J. Org. Chem. 1986, 51, 4440-4446.
- 35) Liu, Y.; Yu, Y.; Gao, J.; Wang, Z.; Zhang, X., Angew. Chem. Int. Ed. 2010, 49, 6576-6579.
- 36) Kim, J.; Jung, I.-S.; Kim, S.-Y.; Lee, E.; Kang, J.-K.; Sakamoto, S.; Yamaguchi, K.; Kim, K., J. Am. Chem. Soc. **2000**, 122, 540-541.
- 37) Amabilino, D. B.; Stoddart, J. F., Chem. Rev. 1995, 95, 2725-2828.
- 38) Mahata, K.; Frischmann, P. D.; Würthner, F., J. Am. Chem. Soc. 2013, 135, 15656-15661.
- 39) a) Glasson, C. R. K.; Meehan, G. V.; Clegg, J. K.; Lindoy, L. F.; Turner, P.; Duriska, M. B.; Willis, R., *Chem. Commun.* **2008**, 1190-1192; b) Zhang, Y.; Crawley, M. R.; Hauke, C. E.; Friedman, A. E.; Cook, T. R., *Inorg. Chem.* **2017**, *56*, 4258-4262.
- 40) Hauser, A.; Vef, A.; Adler, P., J. Chem. Phys. 1991, 95, 8710-8717.
- 41) Clegg, J. K.; Cremers, J.; Hogben, A. J.; Breiner, B.; Smulders, M. M. J.; Thoburn, J. D.; Nitschke, J. R., *Chem. Sci.* **2013**, *4*, 68-76.
- 42) Browne, C.; Brenet, S.; Clegg, J. K.; Nitschke, J. R., Angew. Chem. Int. Ed. 2013, 52, 1944-1948.
- 43) Elmes, R. B. P.; Erby, M.; Bright, S. A.; Williams, D. C.; Gunnlaugsson, T., *Chem. Commun.* **2012**, *48*, 2588-2590.